

# WIRELESS ENGINEER

Vol. XXVII

OCTOBER/NOVEMBER 1950

No. 325-6

## Action and Reaction

**I**N this article we discuss a problem which arose in the discussion following a recent lecture at Birmingham. There are really two distinct problems, both concerned with a homopolar motor. In Fig. 1 the armature consists of an iron cylinder covered with an outer cylinder of copper; at one end there are a number of brushes connected to the positive supply terminal and at the other end a number of brushes connected to the negative supply terminal, so that the armature current is approximately a uniform axial current. The magnet system is cylindrically symmetrical, the field coils being situated at each end as shown. The copper cylinder is situated in an approximately uniform radial field, and will experience a circumferential torque. The armature supply leads are brought out through radial holes in the magnet shell.

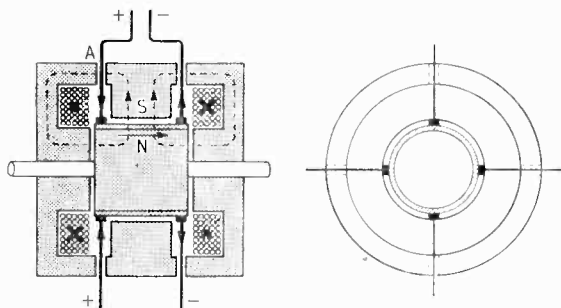


Fig. 1.

The first question is relatively simple; since the magnet system exerts a torque on the armature, there must be an equal and opposite torque exerted on the field system; where and how does this take place? Fig. 2 is an enlarged diagram

of a small portion of the copper cylinder and air-gap, showing the path of a line of force. In the iron of the armature it is radial, but on passing through the current-carrying copper it is curved due to the increasing tangential  $H$ ; in the air-gap the tangential  $H$  is approximately constant and the path therefore straight, but on entering the iron, the tangential  $B$  is greatly increased and the line of force is refracted as shown.

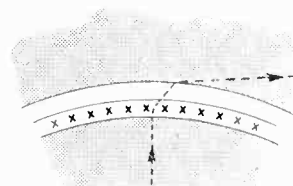


Fig. 2.

As is now well known,\* no tangential mechanical force is exerted on the iron by this refraction of the magnetic flux at its surface. Hence the magnetic flux in the polar ring has a circumferential component, which it loses, however, on passing the leads carrying the current to the armature. We have drawn one set of leads in such a way as to bring out the fact that all these leads and the copper cylinder constitute a solenoid, outside of which there is no circumferential field. Fig. 3 indicates how the current passing through the hole A in Fig. 1 modifies the field so as to remove its circumferential component. The concentrated field on the one side of the hole exerts a transverse Maxwellian pressure on the interface between air and iron, so that the force is not exerted on the conductor but on the iron. This,



Fig. 3.

\**Electrician*, 1945. Vol. 114, p.763.

then, is the answer to our first question; the reaction to the force exerted on the copper cylinder acts on the walls of the holes carrying the armature supply leads.

The second question is of an entirely different character. The axial current in the copper cylinder consists of the movement of free electrons, and due to their axial movement in the magnetic field these free electrons experience a force normal to the field; that is, circumferential with a small inward component. The latter will tend to give the cylinder a negative charge on the inside and a positive charge on the outside, but we are more interested in the circumferential force on the free electrons.

Our second question is this. How are the circumferential force and consequent torque transmitted from the electrons to the atomic structure of the metal? In the ordinary armature conductor the movement of the electrons is limited and a very small movement causes large

electrostatic forces, but in this cylinder the circumferential movement is quite unlimited, so far as the geometry of the conductor is concerned. The most probable explanation appears to be that each axially moving electron is accelerated circumferentially and thus follows a spiral path until it collides with an atom. The torque will then be due to the bombardment of the atoms by the myriads of spirally moving electrons. The only alternative explanation is that, although the so-called free electrons are free to move from atom to atom in the direction of an applied electric field, they are not free to move at right angles to this path but are constrained by electrostatic forces between them and the atoms. If, instead of copper, we assume the armature cylinder to be made of a perfect conductor, the explanation of the torque becomes even more difficult.

G. W. O. H.

---

## Sommerfeld's Surface Wave

**I**N 1909 Sommerfeld published a mathematical article of seventy pages in which he showed that, when a dipole radiates electromagnetic waves over a plane earth, in addition to the radiation into space, there is a surface wave; that is, a wave attached to the surface, and therefore radiating cylindrically rather than spherically. This tends to conserve its energy near the earth's surface, but on the other hand it is subjected to attenuation due to losses in the earth's surface. Although only solved for a plane earth, it was thought that this surface wave was effective in transmitting the waves around the earth's curvature. Zenneck was associated with Sommerfeld in his original work on the subject, and the wave is sometimes referred to as Zenneck's surface wave. The existence of this surface wave was based on the solution of a complex differential equation, and in 1919 Weyl

raised doubts as to the correctness of Sommerfeld's solution. In 1935 Norton gave a solution which contained no surface wave, and in 1937 and 1948 Burrows published experimental results which agreed with Weyl and Norton and disagreed so greatly with Sommerfeld as to show beyond doubt that the surface wave was based on some error. In 1937 both Wise and Rice gave solutions of the problem which did not contain a surface wave.

In the *Proceedings of the I.R.E.* for July there is an article by two scientists working in Paris. T. Kahan and G. Eckart, who have gone into the matter very thoroughly and have discovered that, in carrying out his integration, Sommerfeld neglected a factor which just cancels out the surface wave. The surface wave of Sommerfeld and Zenneck is therefore non-existent.

G. W. O. H.

---

On account of the recent dispute in the printing trade we regret that it has not been possible to publish *Wireless Engineer* on its normal dates. This issue, which is dated October/November, has been expanded to include double the normal number of Abstracts and Reference pages; it includes abstracts which would have normally appeared in the September and October issues.

# INTERFERENCE EFFECTS IN PULSE-WIDTH MODULATION

## *Television Sync-Pulse Sound System*

By W. E. Ingham, B.Sc., (Eng.), M.I.R.E., Grad. I.E.E.

*(E.M.I. Research Laboratories Ltd.)*

**SUMMARY.**—This article describes the results of an investigation designed to determine the effects of ignition interference on a width-modulated sync-pulse method of transmitting television sound.

Emphasis is laid on the importance of considering interference levels which correspond to those normally encountered in practice, and in an experimental study, of using interference inputs having the same character as actual impulsive fields. Great importance is also attached to the choice of the method of measuring the level of the noise output, in order that the result shall agree with the 'loudness impression,' given to the listener, of the noise from the loudspeaker. This article therefore contains details of a suitable subjective method of measurement, and shows how this was developed from a similar method which proved inadequate because it gave only one 'figure of merit' to represent the performance of the system. The method may be used to check the performance of any modulation system.

A limited number of objective noise readings were taken, and from a somewhat brief comparison of these results it appears that r.m.s. output-noise measurements are in agreement with the subjective ones. It seems that, with certain limitations, these objective readings are valid, and should certainly be used in preference to peak value readings.

The results are given of measurements made to show how the noise output is affected by changes in the synchronizing-pulse demodulator. Thus the performance to be expected from any particular circuit may be estimated, and the optimum result obtained. Graphs are also drawn to compare the modulated-synchronizing-pulse system with amplitude and frequency modulation over all interference levels likely to be encountered in normal use.

## 1. Introduction

### 1.1 *W.M. Sync-Pulse Sound*

**B**EFORE dealing with the effects of impulsive interference it is necessary briefly to describe the method of transmitting a television sound signal by width modulating the synchronizing pulses contained in the vision signal. For brevity, the method is here termed 'w.m. sync-pulse sound,' and a detailed description has been given by E. L. C. White.<sup>1</sup>

The sound programme associated with the television picture is transmitted on the same carrier as the vision signal by width modulating the line synchronizing pulses. In common with other pulse-modulation systems, the upper frequency limit of the a.f. modulation is restricted to approximately one-half of the pulse-repetition frequency. It is considered that, with the standard 405-line television signal, this results in a loss of quality that is too great for normal broadcast programme purposes. However, with a 605-line 50 frames/sec interlaced signal, in which the pulse-repetition frequency is 15,125 c/s, the frequency range of the a.f. signal may extend up to about 7 kc/s. Preliminary investigations showed that reasonably satisfactory sound quality could then be obtained.

In a pulse-width modulation system the time duration of the pulse is varied, either increased

or decreased, according to the instantaneous amplitude (positive or negative) of the a.f. modulation.

In this system of line sync-pulse modulation the leading edge of the pulse is unaltered and the position of the trailing edge is varied. This enables the leading edge to be used to synchronize the line time base of the receiver in the usual manner. In the waveform illustrated in Fig 1, the unmodulated synchronizing pulses are of 5  $\mu$ sec duration, the width being varied between 7  $\mu$ sec and 3  $\mu$ sec on 100% modulation.

At the receiver the synchronizing pulses may be separated from the vision signal by the usual sync separator. These mixed pulses then contain

- The required audio modulation frequencies,
- Components of the line sync-pulse waveform,
- Components of the frame sync-pulse waveform,
- Sum and difference frequencies.

It is, therefore, necessary to separate the line synchronizing pulses, carrying the wanted modulation, from the unwanted frame pulses. The line synchronizing pulses are carried on through the frame synchronizing period, so this separation may be accomplished by a gate<sup>1</sup> designed to pass only the required line synchronizing pulses. A low-pass 'receiving filter' will then remove the

MS accepted by Editor, February 1950

unwanted line-pulse components in the usual way, leaving only the desired a.f. signal.

At high carrier frequencies, the interference produced by impulsive noise fields is one of the most important factors in determining the reliable service range of a given transmitter (except in country districts where the limiting factor may be random noise). It was therefore necessary to investigate the performance of this modulation system in respect of impulsive noise.

The experimental data obtained is recorded here in chronological order, as it is then possible to show how the final method of measurement was developed. Brief reference is made to the results as they occur, but as they are best considered in relation to one another, detailed analysis is postponed to the end (Section 4).

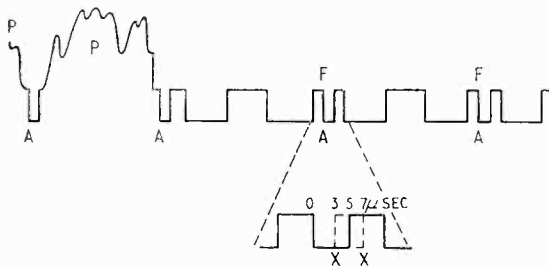


Fig. 1. Vision waveform for width-modulated sync-pulse sound. A = line-synchronizing edge; XX = limits of modulation; P = picture signal; FF = frame synchronizing pulses.

### 1.2 Characteristics of Interference

The various types of 'interference' may be classified under three main headings, namely

- (a) Signals from unwanted transmitters,
- (b) Random fluctuation noise,
- (c) Impulsive interference.

This paper is concerned with the last, but as types (a) and (b) were inevitably encountered, their effects are recorded in brief.

Impulsive interference is the type of interference generated by motor-car ignition systems, electric-traction systems, certain domestic appliances and other devices in which sudden changes of current may occur. Probably the most common source of such interference in television reception is the motor car.

Various estimates of the radiation field, by Eaglesfield<sup>2</sup> and others, suggest that the impulse is of very short duration ( $10^{-9}$  sec). It is also suggested that each nominal spark gives rise to a train composed of a varying number of impulses, and being of variable length<sup>2, 6, 9</sup>, up to 1.5 msec. The impulses vary in amplitude in a random manner,<sup>9</sup> particularly in an ignition system using a number of spark gaps, and it has been shown<sup>11</sup> that commutator interference is of

a similar structure and has a similar random nature.

As the impulses are of such very short duration, they are modified by the relatively small bandwidths existing in the receiver. It has been shown that, provided the impulses appear as separate transients, their output amplitude is proportional, and their duration is inversely proportional, to the bandwidth<sup>5, 6, 13</sup>.

The complex nature of the interference field makes it undesirable to use a simplified impulse generator in an experimental investigation of this type. Relatively long impulses of constant amplitude, for example, should be avoided<sup>16</sup>. They are particularly unsuitable in a system such as this in which the operation of the demodulator may change as the noise input level is varied, as they would tend to show a rapid transition of noise output from one level to another which would not, in fact, occur in actual use. It has also been shown<sup>2</sup> that a spark gap associated with a relatively non-inductive circuit tends to produce a single impulse in place of the normal impulsive train. It is also known that a circuit consisting of an induction coil and a single spark plug, radiates impulses which, though still of random amplitude, vary much less in amplitude than do those from an actual multi-plug motor-car circuit.

Therefore, in order to ensure that results representing the actual performance of the gating and limiting circuits should be obtained, a four-cylinder car-ignition system was used to generate the interference.

### 1.3 Consideration of the Method to be used.

A small transmitter was constructed and provision was made to enable the carrier to be frequency-modulated by the sound signal, or to be amplitude-modulated by either the actual sound signal or a 605-line sync-pulse television signal, in which the line sync-pulses were width-modulated by the sound signal.

The output of the transmitter was mixed with the noise signal, and the combined signal and interference applied to the inputs of two receivers. The first was a communication-type of superheterodyne, which could be switched to receive either amplitude modulation or frequency modulation, and the second was a normal television receiver. The a.f. output from each detector was taken to a common a.f. amplifier (provision being made to reduce the frequency range of the latter by a low-pass filter), and thence to a loudspeaker.

The procedure envisaged was that the gain of each receiver should be adjusted so that, with a given transmitter power and 100% modulation, the a.f. output would be equal

to some predetermined figure which was representative of a normal listening level. The interference signal was then to be applied, and the output noise level noted.

However, as the character of the sound produced by the interference varies with the type of modulation in use, it was first of all necessary to decide on the method to be used to measure the noise output. It was essential that the method should give a result in agreement with the loudness impression of the complex noise sound to the listener.

From published work, it would appear that although many practical and theoretical investigations have been performed in order to determine the effect of various circuit parameters on the shape and magnitude of the output noise impulse, the interpretation of this complex output in terms of true annoyance value has not always met with the attention it deserves. It should be remembered that the final judgment on the noise level rests, in practice, with the listener. Therefore, the measuring device must measure the peak value, the r.m.s. value, or whatever value corresponds to the true 'annoyance value'—if indeed any such single value is found to be adequate. Thus, a meter whose

reading does not represent the loudness correctly may possibly be suitable for obtaining relative readings representing intensities of the same noise, but would give quite misleading readings when called upon to compare the loudness of two different types of noise. This does not necessarily mean that such a meter would even be satisfactory for use with one type of modulation system. For example, it is shown in a paper by Bradley and Smith<sup>14</sup> that on frequency modulation the output noise character may change with a change in level of the interfering field. The interference produces 'clicks' in some instances, and 'pops' (which are far more disturbing) at other times, an effect which is very noticeable in practice.

A further difficulty is that at high ratios of input signal to interference, the meter readings obtained on 'background noise' alone (including hum, random noise, imperfect frame-pulse separation) are no longer negligible compared with the noise to be measured. A meter is then unable to distinguish the significant from the unwanted noise, and gives an incorrect reading. Neither is it possible to use a meter to measure the noise in the presence of a.f. modulation, unless a very high (or low) frequency is used for the latter.

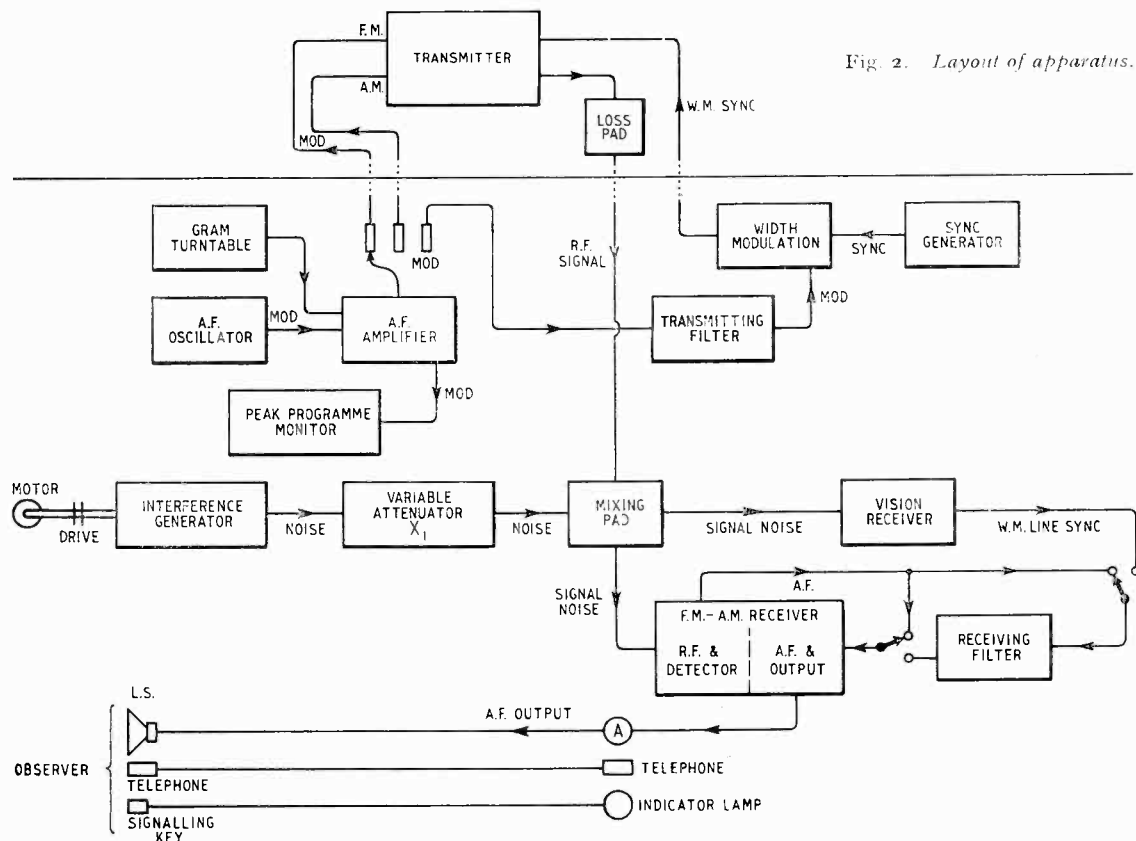


Fig. 2. Layout of apparatus.

It was therefore decided that, rather than attempt to determine the correct objective method of measuring the psychological effect of the noise, a subjective method of measurement should be used in these tests. Some readings were, however, taken using instruments, and although these were not made with the object of fully investigating the problem, they appear to indicate that the r.m.s. value of the noise output is more nearly in agreement with the true loudness level than the peak or mean values. Although the r.m.s. value has previously been used for estimating the level of fluctuation noise, it has not been accepted for use with impulsive noise.

power output being 4 watts at 'black level.' There was no picture present. Fig. 2 shows that the a.f. modulation was applied to the line-synchronizing pulse-width modulator through the transmitting filter. This was a low-pass filter designed to pass frequencies below 6,100 c/s, and is necessary with this type of modulation system in order to prevent unwanted frequency components appearing in the output.

The 'communication receiver' used for the reception of a.m. and f.m. (Fig. 4), employed coupled tuned circuits to give an i.f. bandwidth of  $2 \times 97$  kc/s (6-db points) on f.m., and  $2 \times 17$  kc/s when switched to a.m. A 50- $\mu$ sec demphasis circuit was included on f.m. but not on a.m., the overall audio-frequency response extending to 15 kc/s on the former and 10 kc/s on the latter system. The performance of the f.m. limiter stage was known to be not outstand-

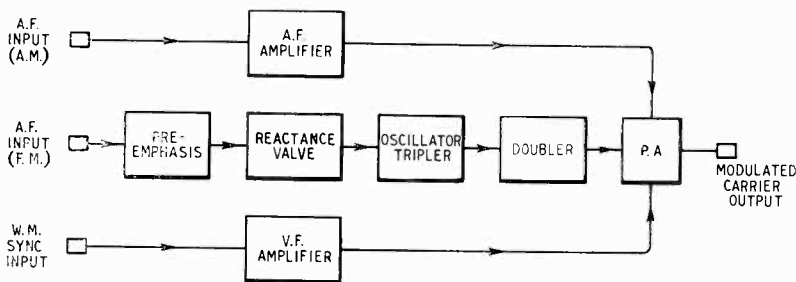
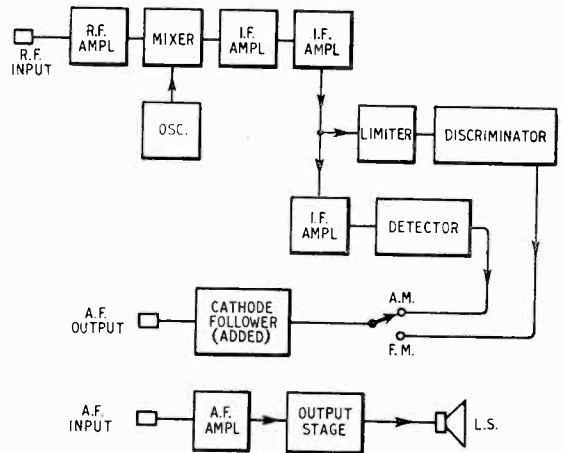


Fig. 3 (left). Block diagram of transmitter.

Fig. 4 (below). Block diagram of a.m.-f.m. receiver.



ingly good. These brief figures are included because the actual results obtained on any modulation system depend to some extent on the characteristics of the receivers employed. However, as these are thought to be fairly representative, they are used here for purposes of comparison.

A television receiver of normal design was used for pulse reception (Fig. 5), the circuits being adjusted to give single-sideband working with an i.f. bandwidth of approximately 3 Mc/s. In the initial experiments a simple demodulator was added, the mixed synchronizing pulses obtained from the normal sync separator being

## 2. Initial Tests

### 2.1 Apparatus

A diagram showing the layout of the apparatus is given in Fig. 2.

The interference generator, formed of the four-plug car-ignition circuit, was housed together with its large capacity accumulator in a heavy copper box. The output was developed across a 10-ohm resistor in the plug circuit, and was brought out to the attenuator via a short length of lead-covered cable. The distributor was driven by a small induction motor at a speed giving about 93 sparks per second.

The attenuator was used to control the interference level, frequent checks being made to ensure that the level of the interference voltage obtained at any given setting was constant. The attenuator was made up from a screened piston-type variable capacitance (4.5 pF to 0.1 pF).

Fig. 3 shows a block diagram of the transmitter which was screened and located about 100 feet from the receivers in order to minimize the pick-up of stray radiation fields. The operating frequency was 45 Mc/s.

A carrier power of 4 watts was used on f.m., with a maximum deviation of  $\pm 75$  kc/s, and 50- $\mu$ sec pre-emphasis. Anode modulation of the final stage provided an a.m. signal, the power being as for f.m. There was no pre-emphasis.

It was also possible to grid-modulate the final stage with the 605-line vision signal, the r.f.

applied to a line-synchronizing pulse 'gate' of the coincidence type, employing a double-triode valve with a common anode load as shown in Fig. 6. A gating pulse was taken from the screen

fully-modulated (7  $\mu$ sec) pulse and reject the following frame pulse.

Fig. 7(b) shows the waveform of the output of the double-triode stage, and it is such that it was possible to separate the modulated pulses on an amplitude basis in the following amplifier. The output was finally applied to a low-pass filter to remove all frequency components other than the wanted modulation.

When this receiver was used in the presence of noise it became apparent that the performance of the w.m. sync system was very unlike that of the a.m. and f.m. systems, and that it would be necessary to repeat the readings with a demodulator which would allow a more detailed investigation to be made.

A more flexible circuit was therefore constructed in addition, in order to allow the various circuit parameters to be varied independently. A cathode follower was added to the receiver (Fig. 5) to supply the complete synchronizing pulses to the new demodulator chassis (Fig. 8).

This was connected to replace that part of the circuit shown (Fig. 2) between the vision receiver and the audio output stage. The synchronizing pulses were amplified and applied to a window circuit consisting of a pair of valves with a

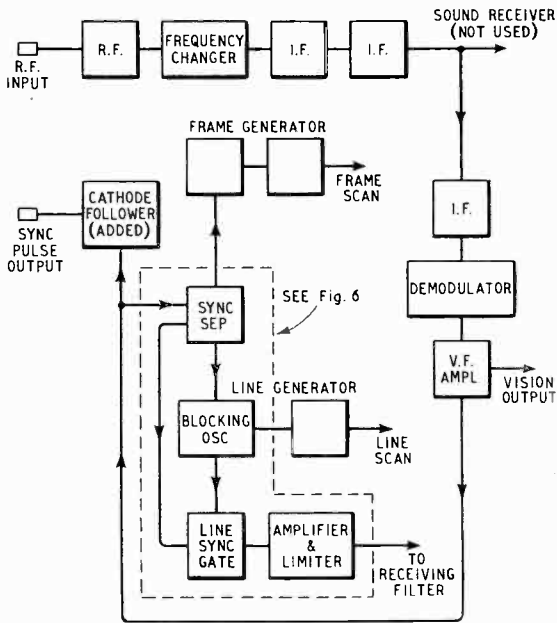
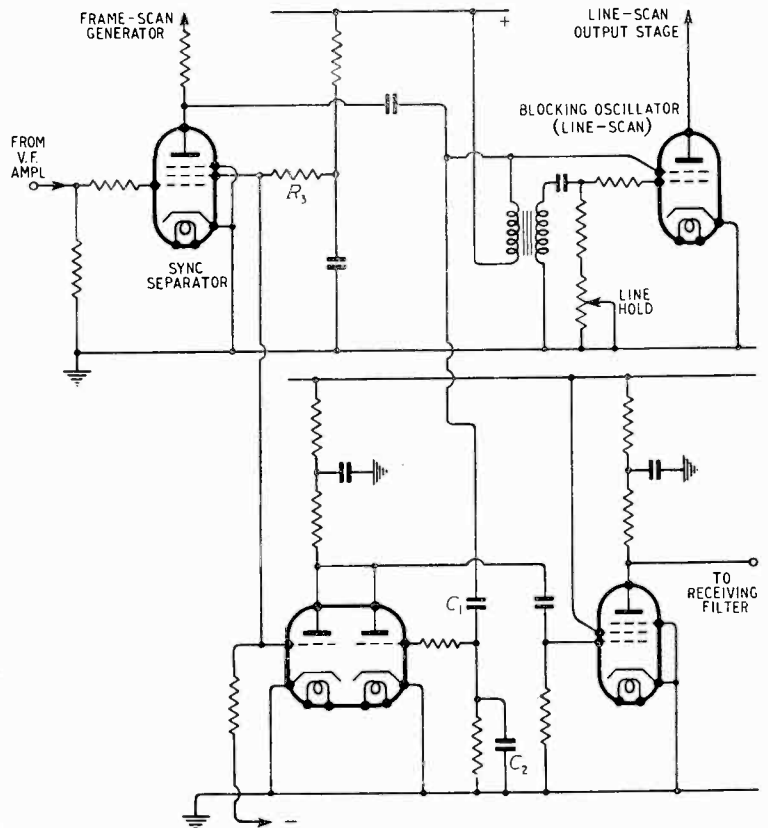


Fig. 5 (above). Block diagram of vision receiver (with modifications.)

Fig. 6 (right). W.M. sync-pulse gate (see Fig. 5).

of the valve used as a line oscillator and was applied through the capacitance potential divider  $C_1C_2$  to the second grid of the double triode. This pulse, illustrated in Fig. 7(a), was limited by grid current and by anode current cut off, so that a slice of the pulse was used, as shown. The waveform of this pulse will be seen to be very suitable as it was of approximately the correct duration. With the circuit used there was a time delay of about 1.5  $\mu$ sec between the leading edge of the synchronizing pulse and the gating pulse when adjusted by 'line hold' to be a minimum. Such a delay introduces no audio distortion unless it is large enough to reduce the excursion of the modulated edge of the synchronizing pulse at full modulation. The trailing edge of the gate must accept the



common cathode circuit of relatively high impedance,<sup>21</sup> by which it was possible to select a 'slice' of about one fifteenth of the amplitude of the synchronizing pulse at any position from top to bottom of the pulse. The slice was then applied to a gate circuit consisting of a similar pair of valves, so that when the gate was closed it was impossible for any input voltage to appear at the output.

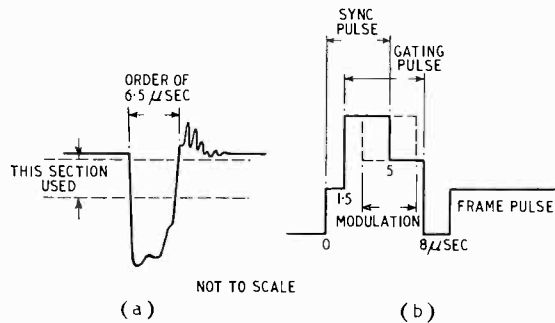


Fig. 7. (a) Gating pulse from line oscillator; (b) waveform of the output from the pulse separator.

By selection on  $S_{1a}$  and  $S_{1b}$  the gating pulse could be obtained

- (i) From the receiver line oscillator as previously explained, Fig. 7 (a).
- (ii) From a multivibrator triggered by the line oscillator.
- (iii) From the multivibrator triggered by a pulse derived directly, over a separate line, from the synchronizing-pulse generator at the transmitter.

This pulse generator was designed to provide a trigger pulse, the timing of which could be continuously varied (either advanced or delayed) with respect to the line-synchronizing pulses. This enabled the position of the gating pulse to be moved [see (iii) above].

The gate width could be altered (by means of the multivibrator) so that there was complete control of the gating conditions.

Switch  $S_2$  (Fig 8) selected either

- (i) W.M. sync-pulse sound.
- (ii) f.m. or a.m. with the receiving filter to limit the audio range.

or (iii) f.m. or a.m. without the receiving filter.

By means of  $S_3$  it was possible to include an amplifier stage with a weighted frequency characteristic (see Section 3.1).

The loudspeaker employed in the subjective tests consisted of either a loudspeaker combination of two moving-coil units for the lower frequencies and a ribbon speaker (horn loaded) for the higher frequencies, or of a single moving-coil speaker of wide range.

## 2.2. Experimental Procedure.

The transmitter output was set up to the level given in Section 2.1, and, on 100% modulation, the gain of the receiver was adjusted to give a fixed output current (on ammeter A, Fig. 2) from the a.f. amplifier. As the attenuators and mixing pads were adjusted so that the gain setting and audio output were normal, this procedure ensured that the receivers were operated under representative conditions. The interference was then applied to the unmodulated carrier through the attenuator  $X_1$ .

The interference input level was then reduced until an observer, listening near the loudspeaker, signalled that the noise output was no longer audible. A similar observation was then made by increasing the interference level, and to improve the accuracy many readings were taken by different observers. Thus for each system under test a reading of the attenuator was obtained, which was a capacitance representing the interference level required, with that

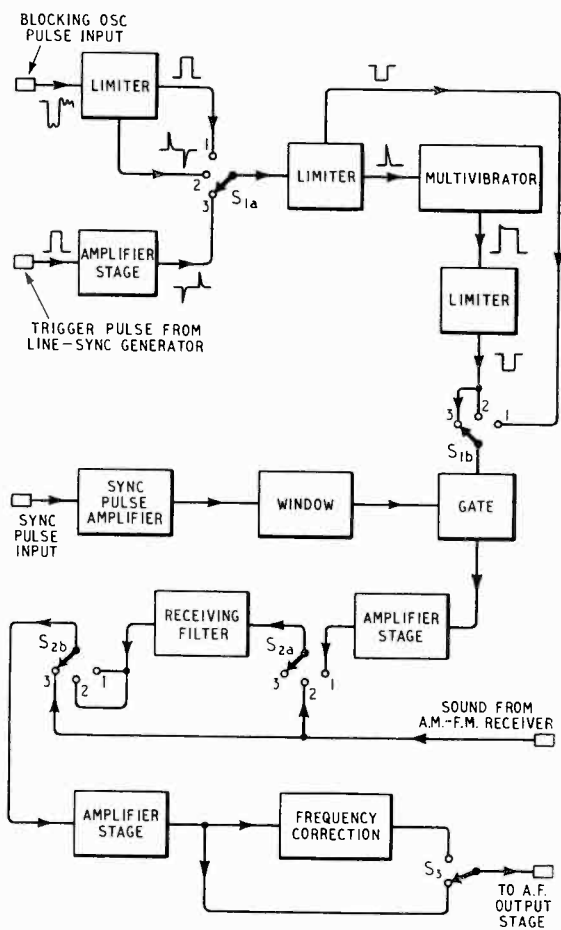


Fig. 8. Block diagram of experimental w.m. sync-pulse demodulator (showing waveforms).

system of modulation, to give a noise output which was just audible.

### 2.3 Results and Limitations of the Method.

It was originally intended that such a reading should be taken to indicate the performance of each method of modulation in respect of impulsive noise. However, the known non-linear relationship existing between the input and output noise levels proved to be so noticeable over the range of interference levels normally encountered, that this scheme had to be abandoned.

If any single 'figure of merit' is used to represent the performance of a modulation system it is likely to be very misleading, as it may only illustrate the performance correctly at one certain input level. In particular, the readings mentioned above have the additional disadvantage that they refer to the input noise levels. If one system is said to be  $x$  db better than another, a comparison of noise outputs is suggested, but with the above readings it would really represent a ratio of interference inputs for a given noise output, which may evidently be quite a different thing.

The readings are therefore not given here in detail, but will be considered in general so far as they illustrate the effects mentioned above.

It was found that, when the simple pulse demodulator (Fig. 6) was used in the initial readings, although the a.m. reading was approximately 20 db higher than that for f.m., very similar attenuator settings were recorded for a.m. and w.m. sync sound (without modulation). These results would therefore have given the impression that the performances were similar in respect of impulsive noise. However it was apparent that whereas the noise appeared gradually on a.m. as the interference input was increased, it appeared suddenly on sync sound when a threshold input was exceeded, so that a further large increase in input was required on a.m. to give an equivalent noise output.

This effect was also shown by the measurements made in the presence of audio modulation. The modulation was chosen so as to mask the noise (a steady tone was found to be quite unsuitable), and to be of approximately constant level. It was then necessary to increase the interference input level in order to make the noise audible over the modulation. The increase required on w.m. sync sound was very small because of the rapid rise of noise output at this point, and was much less than that required on a.m. so that the ratio of noise inputs became about 28 db.

The increase on f.m. was also smaller than a.m. because of the clearly audible increase of noise

output occurring when the signal was frequency modulated<sup>11</sup>.

The pulse demodulator of Fig. 8 was used in order to show the effect of varying the window position, and as these results helped to complete the picture of the operation of the system (Section 4) they are given below. The gate was triggered by the line-synchronizing pulse generator, the delay being adjusted so that the leading edges of the gate pulses and the sync-pulses were coincident at the gate. The gating pulse was adjusted to be  $7\mu\text{sec}$  wide so that it would accept a fully modulated sync-pulse, although no audio modulation was present. The readings are shown in graphical form in Fig. 9, each reading being, as before, an average result of the noise input required for the output to be just audible. The interference input levels are plotted in decibels with reference to the level required with

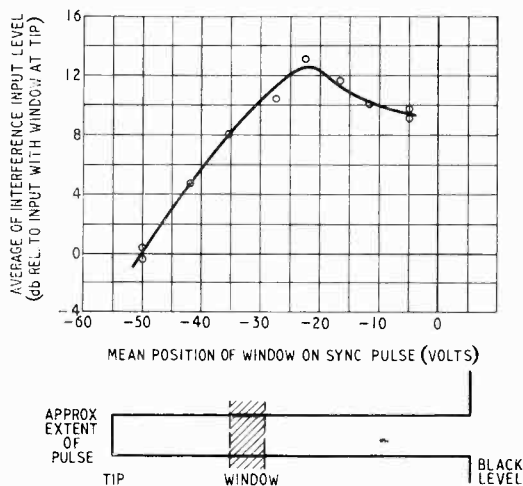


Fig. 9. Graph of noise input required to give just audible noise output at various window positions.

the window at the tip (i.e., zero carrier end) of the synchronizing-pulse, (-50 V, see Fig. 9).

It has been suggested<sup>18</sup> that when a gating circuit is used in connection with a pulse-modulation system, the interference may cause additional noise by affecting the timing of the gate. Readings were taken to check this, by making observations with the gate derived, in turn, directly from the blocking-oscillator pulse (normal), from the multivibrator triggered by the blocking-oscillator, and from the multivibrator when synchronized over a direct line with the line-synchronizing pulse generator (fixed gate). The average results were all within  $\pm 1$  db and no conclusive evidence could be found of additional noise output due to gate shift at this interference level.

Attempts were made, by reducing the bandwidth of the sync-pulse amplifier of Fig. 8, to decrease the height of the noise impulses so that they no longer cut across the window. The demodulator was set up as for the readings of Fig. 9, and the bandwidth altered first with the window at the centre of the pulse and then when almost at the tip (actually - 45 V). The average results are given in Table 1.

**TABLE 1**

Interference Input v. Bandwidth of the Synchronizing Pulse Circuits.

Bandwidth of sync-pulse amplifier stage	Average result for reading attenuator $X_1$	
	Window at - 27 V	Window at - 45 V
Normal	6.3 mpF	2.4 mpF
Reduced to 1.4 Mc/s	8.1 mpF	
Reduced to 0.9 Mc/s	8.9 mpF	2.5 mpF

Other readings either yielded no conclusive result or were repeated in Section 3, so the results are not given. For example, no change in noise reading was obtained when the receiving filter was included on a.m. and f.m. to limit the bandwidth, either in the presence of, or without, modulation. Nor was any change in the w.m. sync reading obtained when, with the window set to the centre of the sync-pulse, the gate width was altered from 4  $\mu$ sec to 10  $\mu$ sec.

The relevant results are examined, in conjunction with those of Section 3, later in the paper.

### 3. More Detailed Tests

#### 3.1 Improved Subjective Method.

Attempts to provide more detailed results, by comparing the noise outputs of the three systems at various interference levels with a steady reference tone, failed owing to the widely different character of the sounds. The following subjective method of measurement was therefore devised, in which the layout of the apparatus (as shown in Fig. 2) was modified according to Fig. 10, and the procedure was as follows.

The gain of the receiver under test was adjusted as before, to give a fixed output on a fully modulated signal (1500 c/s). The output to the loudspeaker was then turned on and off at random by means of the fader, and the level gradually reduced by the attenuator  $X_2$ . The observer caused the signal lamp L to light whenever he considered he was able to hear the modulation, the reading of  $X_2$  being noted at the point at which the observer was just unable to give consistently correct signals. This figure represented the sound output on 100% modulation.

Similar figures were obtained for the various

noise outputs resulting when different interference levels were applied to the unmodulated carriers. Readings were taken by two observers, and the average value calculated. A graph was then plotted to show the law relating interference input to noise output for each modulation system. The position of each of these graphs was fixed with respect to the sound output on full modulation, and therefore the graph of one system can be compared with the graph for any other system.

Any hum output was made inaudible by means of the 200-c/s high-pass filter, frame synchronizing pulses being removed so as to avoid any slight noise due to possible imperfect suppression. A further source of error was removed by means of a frequency-correction network. This was a stage with a frequency response weighted to represent the difference between that of a normal ear at threshold, and at 60 db above threshold. The network had zero gain at 1,500 c/s. When the correction amplifier was in circuit, the noise appeared to the ear to have the same frequency distribution at threshold as at the normal listening level, which was assumed to be 60 db above threshold.

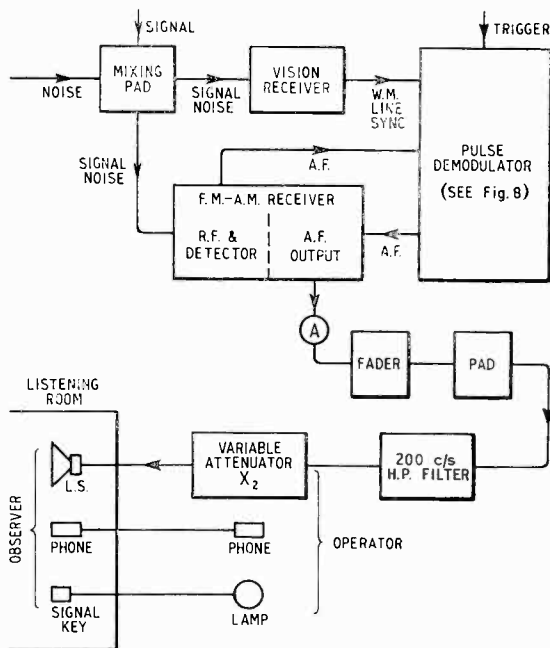


Fig. 10. Modified layout for more detailed measurements.

#### 3.2 Results Obtained by the Improved Method.

The amplitude and frequency modulation readings are included in Table 2, where it will be noticed that the readings of two observers are recorded in full to illustrate the procedure involved, in subsequent readings only the resulting

graph is given, but it should be remembered that the same method of averages was used throughout. No low-pass receiving filter was used on these runs, and there was no audio modulation present on the signal.

Specimen readings were repeated on separate occasions (by way of a check) for each set of results, although these also are not shown. As the absolute level of the interference input was unknown, the readings were recorded on an arbitrary decibel scale, Fig. 11 showing the results in graphical form.

Similar readings were then taken for w.m. sync sound, the transmitter and receiver being set up as before, and input-output graphs obtained for three different adjustments of the pulse demodulator gate. Condition 'N' (normal)

gave the same result as 'F.G.' (fixed gate)—within the limits of measurement. Although the average value tended to be less, the change was not sufficiently large to assess by this method. The threshold input (for Condition 'F.G.') was determined by the earlier subjective method, described in Section 2.2, as the noise output at this input was below random noise level (see Fig. 12). With  $X_2$  set for an output level of 76 db below 100% modulation, the average reading of  $X_1$  was 3.5 mpF, corresponding to 21.5 db on the input scale. These results are plotted on Fig. 12, with a.m. and f.m. recorded for comparison,

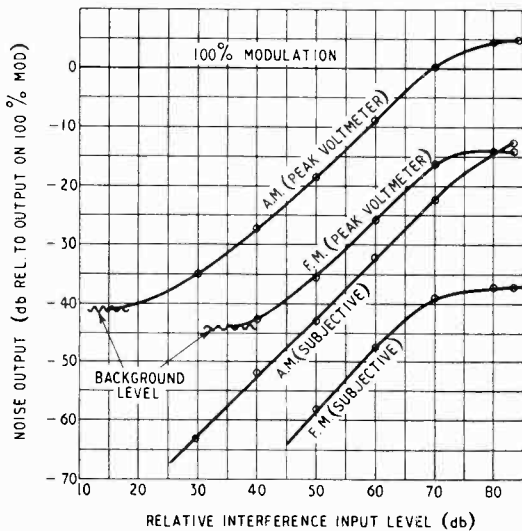


Fig. 11. Interference input and noise output for a.m. and f.m.

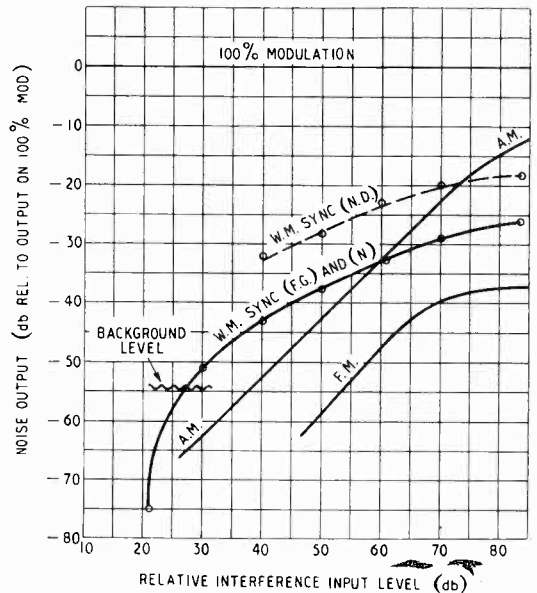


Fig. 12. Interference input and noise output for w.m. sync sound (f.m. and a.m. for comparison); w.m. sync gate adjustment: F.G. = fixed gate; N = normal; N.D. = Normal, but gate delayed.

TABLE 2

Noise Output v. Interference Input (A.M. and F.M. readings).

Interference input level		Noise Output								
$X_1$ (mpF)	Rel. Level (db)	Amplitude modulation				Rel. to output on 100% Mod. (db)	Frequency modulation			Rel. to output on 100% Mod. (db)
		Attenuator Reading $X_2$ (db)			Obs. A		Attenuator Reading $X_2$ (db)		Average	
		Obs. A	Obs. B	Average			Obs. A	Obs. B		
4500	83.5	94	92	93	-13	70	68	69	-37	
3000	80	92	92	92	-14	70	68	69	-37	
1000	70	84	84	84	-22	68	66	67	-39	
300	60	74	74	74	-32	60	58	59	-47	
100	50	64	62	63	-43	50	46	48	-58	
30	40	54	54	54	-52					
10	30	44	42	43	-63					
100% modulation		106	106		0	106	106		0	

and they show that with the gate obtained from the blocking oscillator, and the line-hold control incorrectly adjusted—Condition 'N.D.' (normal, delayed)—there was additional noise output due to gate shift.

It may be seen that at the worst input signal to interference ratio considered, the noise output on w.m. sync sound was about midway between the outputs obtained on amplitude and on frequency modulation. Although the sounds were characteristically different—for example the noise on w.m. sync sound appeared much more 'broken' and 'uneven' than the relatively steady note on a.m.—it was generally agreed that this corresponded with the aural impression obtained by switching quickly from one system to another.

The graphs also show that at some interference level the output noises on a.m. and w.m. sync sound will appear equally loud. It was thus possible to make a more precise check by reducing the interference level until an observer, listening normally, signalled that this point had been reached. The comparison was facilitated by arranging for a quick change-over by switching the loudspeaker from one receiver to the other. The readings of the capacitance attenuator  $X_1$  obtained in this way are given in Table 3.

**TABLE 3**

Interference Input Required for Equal Noise on A.M. and W.M. Sync Sound.

Reading of Capacitance attenuator $X_1$ (mpF)
310
270
350
250
320
235
Geometric mean 288

**RESULT.**  
288 mpF on  $X_1$  corresponds to 59.5 db on the arbitrary (decibel) input scale.

It will be seen that the average agrees with the point of intersection of the two graphs (Fig. 12).

The way in which the noise output varied with change of the window position was also determined at various levels of input interference. The transmitter and receiver were adjusted as before, the average results being plotted graphically on Fig. 13. The threshold interference input levels were measured as for curve FG (Fig. 12) with  $X_2$  set for an output level of -76 db. Substantially the same input was required with 30 db more a.f. gain showing that a sharp noise cut off was obtained at this input.

The changes in gate width and circuit frequency response previously made in Section 2.3 were repeated, this time with the object of noting the corresponding variation in noise output at high interference levels. The subjective readings, how-

ever, failed to reveal any conclusive change of output noise level.

### 3.3 Objective Noise Measurements.

Some of the previous tests were also carried out by making objective readings of the output noise level. In the first instance a peak-reading programme meter having a short charging time constant and long discharge time was used. The audio bandwidth of the meter was greater than that of the receiver, and care was taken to work at a constant low deflection to avoid overloading.

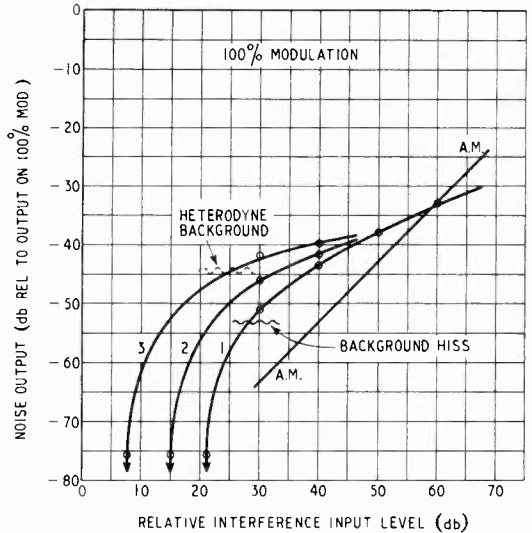


Fig. 13. Variation of noise output with window position; 1. window at -28.5 V; 2. window at -42 V; 3. window at -56 V; (a.m. for comparison).

The meter was substituted for the loudspeaker and a constant deflection maintained by means of the attenuator,  $X_2$ , the reading of the latter being noted for each interference input level. Readings equivalent to the subjective results of Table 2 are shown on the same graph (Fig. 11).

The noise output was also measured by noting the current output delivered by the receiver to a resistive load. The readings were taken at a low signal-to-interference input level, in order to avoid errors due to hum and random noise.

A rectifier meter, reading mean value (calibrated r.m.s.), was used in the first instance, followed by a thermo-type meter to give the r.m.s. value. The a.m. and f.m. readings are given in Table 4 (a), except the current output on f.m., which was not large enough to be measured on the square-law scale of the meter used. Table 4 (a) also gives similar results for the w.m. sync-pulse system, under the three receiver conditions noted in Section 3.2.

As previously mentioned, no detailed attempt was made to determine conclusively the correct objective method of noise measurement. How-

ever, it should be noted that the results of Table 4 do appear to indicate that the r.m.s. value is more nearly in agreement with the subjective results than the peak or mean values. For example, according to the readings obtained using the peak-reading meter, at high interference levels the noise output exceeds the signal output on 100% modulation (Fig 11). A simple listening test showed that this was very far from the impression obtained by ear. Further, the general shape of the input-output graph is not the same as that obtained by subjective measurement. The errors due to 'background noise' at high signal to noise inputs are also shown, and these errors may be expected to be worse when an r.m.s. meter is used.

The noise outputs, obtained at maximum interference input by measurements yielding mean and r.m.s. values, are compared in Table 4(b) with the subjective ratios taken from Fig 12. The mean value readings give the correct answer only when used to compare the levels of noises

**TABLE 4(a)**

Noise output—Mean and R.M.S. Value Readings.

Modulation system	Noise output current (mA) at maximum interference input	
	Mean value	R.M.S. value
A.M.	4.1	8.5
F.M.	0.22	—
W.M. sync (F.G.)*	0.45	2.23
W.M. sync (N.)*	0.36	1.7
W.M. sync (N.D.)*	0.91	4.85

\* See Fig. 12.

**TABLE 4(b)**

Comparison of Subjective and Objective Noise Output Readings.

Modulation systems compared	Ratio of noise outputs at maximum interference input (nearest db).		
	Mean value readings Table 4(a)	R.M.S. readings Table 4(a)	Subjective reading Fig. 12
Amplitude mod	25	—	24
Frequency mod			
W.M. Sync (N.D.)	6	7	8
W.M. Sync (F.G.)			
W.M. Sync (F.G.)	2	2	0
W.M. Sync (N)			
Amplitude mod	13	5	5
W.M. Sync (N.D.)			
Amplitude mod	19	12	13
W.M. Sync (F.G.)			

of a similar character. For example, the readings are correct when comparing various outputs on w.m. sync sound, but not when the noise output for this system is compared with that for amplitude modulation. In the latter instance the noises sounded completely different, and it would appear that the ear rates the annoyance value on a power basis. The readings show that the ratios of the levels, as assessed by the ear, correspond in every case with the ratios of the r.m.s. values of the output currents.

On the basis of these results it was felt that it would be correct to use an r.m.s. reading meter to measure those changes of noise output which had proved too small to measure subjectively; for example, inconclusive results were obtained previously when attempts were made to measure aurally the effect of a change of gate width. The tests did show, however, that the noise was always of a similar nature, and therefore accurate results could certainly be expected if r.m.s. meter readings were taken using high interference levels to avoid errors due to background noise.

The thermo-junction meter was used to measure the noise output current. The gate width was then varied over the same range as for the subjective test, the corresponding outputs being recorded in Table 5. The results show that there

**TABLE 5**

Noise Output v. Gate Width.

Gate width (μsec)	R.M.S. Noise output current (mA)
10	1.5
7	1.5
5	1.5
4	1.25

was no apparent change in noise output until the gate width was reduced so far that it no longer included all the synchronizing-pulse.

Although the purpose of the investigation was to determine the performance of w.m. sync sound with regard to impulsive noise, some objective readings were also taken of the random background noise level. No particular effort had been made to design for optimum performance in this direction, so the level may not be taken as necessarily indicative of a representative figure. The results did, however, give a check on the distribution of the noise, and on the reading obtained subjectively during the impulsive noise output measurements (Figs 12, 13).

The readings are recorded in Table 6. A thermo-junction meter was again used, the setting of the attenuator  $X_2$ , and the meter reading, being noted for the output on full modulation and on the noise to be measured.

The noise level relative to full modulation was then calculated, and is given to the nearest decibel. Although a high degree of screening was used, beat notes due to r.f. carrier interference were obtained, as the field strength of the unwanted interference was high. This output was also measured and the readings indicate how the effect of such interference may be minimized.

When the thermo-junction was used in the measurements of impulsive noise outputs [Table 4(a)], it was not possible to measure the low f.m. output level. However, because of the extra gain provided for these 'background noise' readings it was now possible to rectify the omission by employing the method used to read the background levels. This result, showing the noise output at maximum interference input, is included at the end of Table 6(f), and is in agreement with the previous subjective reading of Table 2.

#### 3.4 Impulsive Interference on Vision.

During this investigation the absolute field strengths of the interference fields were not known, but this was not important in view of the way in which the levels were set up. The fact that the interference input was adjusted experimen-

tally, with normal signal strength and receiver gain, so that all reasonable noise output levels were produced, ensured that practical interference field strengths were investigated. However, in order to relate the performance of the w.m. sync sound channel to the performance on vision, the interference produced on the picture raster was noted at several interference levels. The particular vision receiver in use had no peak limiter or other suppression device.

The brightness control was advanced until the raster was just visible (no picture being present), and the transmitter and receiver gains were adjusted in the usual way. It was observed that the raster suffered heavy interference with  $X_1$  set at 4500 mpF, producing an interference level of 83.5 db, the white spots then being defocused owing to the large amplitude of the noise impulses. Slight displacement of individual lines could be observed. When the interference level was reduced to the equivalent of 50 db on the input scale the white spots were quite small and relatively few in number, and it is believed that with a picture present they would have been unnoticeable at an interference input level of 34 db.

**TABLE 6**  
Level of Random "Background" Noise on W.M. Sync Sound.

Adjustment of demodulator				Loss at $X_2$ (db)	R.M.S. Output current (mA)	Noise level relative to 100% mod. (nearest db)	Nature of noise	
Gate trigger	Gate width ( $\mu$ sec)	Gate position	Window position (see Fig. 9)					
A	From line-sync pulse generator.	7	Delay on gate leading edge very small.	-22.5V	8	4.3	-53	Random hiss.
B	From line-sync pulse generator.	7	Delay on gate leading edge very small.	-50V	18	4.2	-44	Heterodyne beats.
C	From blocking oscillator.	6.5	"Line hold" adjusted for minimum delay.	-22.5V	16	3.9	-46	Random hiss.
D	From line-sync pulse generator.	4	omitting both pulse edges.	-22.5V	0	1.7	-70	Random hiss.
		5	omitting pulse leading edge.		8	4.5	-53	
		5	omitting pulse trailing edge.		8	3.7	-55	
		7	including both pulse edges.		14	3.8	-49	
E	From line-sync pulse generator.	7	Delay on gate leading edge very small.	-22.5V	62	4.1	0	Signal output (100% modulation.)
F	Frequency modulation.				26	3.9	-36	Impulsive interference.

## 4. Discussion of Results

### 4.1 Behaviour of W.M. Sync Sound System.

The original impression obtained on listening to the noise output as the interference level was increased, was that the noise output appeared abruptly at a particular input—the threshold input, and that above this input there was only a relatively slow increase in output. This was mentioned in connection with the earlier readings (Section 2), and is upheld by the measured performance figures of Fig. 12.

The fact that the input-output graph is non-linear shows how important it is that such an investigation should be performed over a suitable range of input signal-to-interference ratios, and how both theoretical investigations and practical experiments involving objective noise measurements, must be checked to ensure that practical signal-to-noise ratios are considered. The results also show that at all but very high input signal-to-interference ratios, the noise impulses are large compared with the carrier amplitude. This is partly because of the relatively large bandwidth of the synchronizing-pulse circuits, but it does emphasise the fact that a theoretical study considering peak voltages which are, at a maximum, only equal to the signal amplitude, will give an incomplete picture of the operation of the system.

The reason for the appearance of an interference threshold is that, for inputs below this value, the impulses are of insufficient amplitude to reach the part of the synchronizing pulse admitted by the window circuit. They therefore cause no noise output. As their amplitude increases the larger ones break across the window area, and if the interference consisted of uniform rectangular pulses the output would increase no further than that reached when they extended right across the window space. The action with the true noise impulses is similar, so that the noise output does not increase in proportion to the interference input. Fig. 12 shows the sort of rise to be expected.

Depending on the relative amplitude and phase relationships existing at its arrival, a noise transient may either effectively increase or decrease the amplitude of the carrier. Thus, noise impulses may be produced which run either 'inside' or 'outside' the synchronizing pulse, as shown at A and B respectively (Fig. 14). This diagram is drawn assuming positive modulation at the transmitter, as used in these tests. The most important impulses from the point of view of output noise are the larger and more numerous ones shown at A, which arise when the carrier amplitude is increased.

This is illustrated by the readings taken to show the variation in threshold input with change of window position (Fig. 9). They show that the optimum position for the window, though towards the middle of the pulse, is nearer the 'base' (X) than the 'tip' (Y). The readings of noise output (Fig. 13) show that if the window is moved away from the tip, no improvement will result at high or even medium interference levels, because the impulses are large and extend the whole length of the pulse. However, at highest signal-to-noise inputs, when the noise output is of the order of 40 to 50 db down on the modulation, the position of the window is of some importance. Here it was possible, with the circuit in use to reduce the noise by about 10 db when the window was moved away from the tip. The variation in the position of the threshold input was very marked (Fig. 13), an improvement of about 14 db being obtained. This figure is in agreement with the subjective ratio obtained previously (Fig. 9), although the output of the noise generator was modified between these readings so that the actual readings of  $X_1$  were not the same. Fig. 9 also shows how the threshold noise input is lower with the window at the tip than at the base of the pulse. These improvements are useful as w.m. sync sound performs less satisfactorily, in relation to a system in which noise output is proportional to interference input, at these higher input signal-to-noise ratios than at high interference levels.

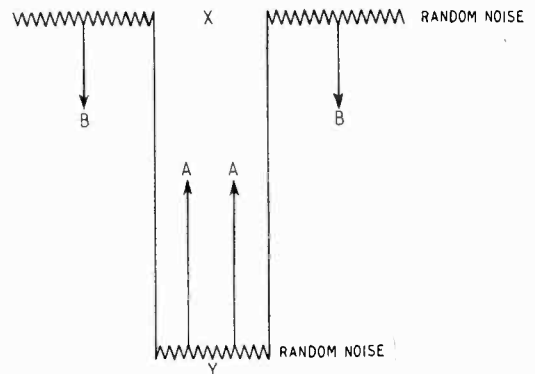


Fig. 14. Synchronizing pulse with interference.

The readings taken to show the effect of a variation of gate width also support this noise distribution theory. Although the actual readings are not given, those of Section 2.3 were in agreement with the repeated tests of Section 3.2 in showing that, with the window at the optimum position, any change of output level for gates between 4 and 10  $\mu$ sec is smaller than can be measured subjectively. The objective readings

of Table 5 confirm this. They show that the output is indeed not reduced until the gate is made small enough to reject a part of the synchronizing pulse. The noise impulses 'outside' the pulse are relatively few in number and are limited to an amplitude which makes them insufficient to affect the noise output. Further, the reduction in noise output obtained by accepting only  $4 \mu\text{sec}$  (or 0.8) of the pulse width is about 1.6 db, which (allowing for error in reading random noise impulses) is in agreement with the 1.9 db predicted by assuming the output to be proportional to the gate width. Thus, if the timing of the gate is delayed by up to  $3 \mu\text{sec}$  compared with the synchronizing pulse, the modulation would not be affected, but the noise may be expected to fall in the ratio 5 : 2; i.e., by 8 db.

Such a large delay, although theoretically possible, would be impracticable in normal use, but some improvement may be obtained in this way. It will be noticed that the delay introduced when the blocking oscillator was used ('N' Table 4) reduced the noise output below the level obtained when the whole synchronizing pulse was accepted ('F.G.'). The blocking-oscillator anode pulse appears to be very suitable for use as a gating pulse for the following reasons

- (i) Using a transformer and circuit of normal design, the pulse is of approximately the correct duration.
- (ii) Impulsive interference does not seem to give rise to additional noise output by affecting the gate timing.
- (iii) The circuit may be arranged to provide the delay necessary to reduce the impulsive noise output.
- (iv) The delay also reduces the random noise.

That the noise output is not normally increased by gate shift (ii) above, was shown by the readings of Section 2.3, and of Section 3.2 (see Fig. 12). Those of Section 2.3 (which it will be remembered were readings of interference input level), were constant (within  $\pm 1$  db), but as these readings were taken at low interference input levels no gate shift would be expected. However, the same result was obtained at very high interference levels when the 'line-hold' control on the receiver was correctly adjusted, so that the normal curve 'N' (Fig. 12) was the same as with a fixed gate ('F.G.', Fig. 12). When however, it was not correctly adjusted, the noise output was increased by as much as 10 db ('N.D.', Fig. 12).

Although, on the above showing, gate shift does not appear to be a likely source of noise, it is worth noting that the line oscillator was triggered from the tip of the synchronizing pulse

in the above tests, and that there was no audio modulation present. It would seem that this type of noise may be more likely to occur at high modulation depths, as less shift may then be tolerated before noise output results, although of course the noise would be less noticeable. This idea was not checked but, if required, a further improvement could be obtained by triggering the gate from the output of the window circuit, and by so doing, other unwanted noise levels could be reduced as was shown by 'A' and 'C' in Table 6. These readings show that changing the gate from the line-synchronizing pulse generator of the transmitter (A), to the blocking oscillator of the receiver (C), increased the noise level from 53 db to 46 db below 100% modulation because of the resulting heterodyne beats. The window was unchanged, so that the same portion of the synchronizing pulse was demodulated in C as in A. That this continuous-wave interference was located at the tip of the synchronizing pulse was checked by reading B, in which the gate was fixed as in A, but the window moved to the tip. The noise (heterodyne beats) gradually appeared as the window was moved to the zero carrier end. Thus, had the blocking oscillator been triggered from that part of the pulse seen by the window circuit, the noise would have been removed by the usual correct adjustment.

It appears that no great improvement may be obtained by a reduction of the bandwidth of the stages before the window, although the effect of this experiment was reduced by the rather limited bandwidth of the vision receiver. The subjective readings of Section 3.2 showed no reduction in output noise level at high interference input levels, and remembering how the investigation indicates that the interference impulses are of large amplitude, none would be expected. Readings taken at low noise inputs (Table 1) indicate that some small improvement of the threshold input may be realised by keeping the bandwidth low when the window is at the centre of the synchronizing pulse. The readings also verify that there can be no improvement when the window is at the 'tip' of the pulse, as even small noise impulses will then give rise to a noise output. The degree of improvement possible in this direction is very limited because of the deformation of the synchronizing pulse which is produced, and eventually leads to excessive audio distortion.

In connection with the blocking oscillator it was mentioned that a delay on the gate pulse reduces the random background noise. This results because the noise carried on the unmodulated leading edge of the synchronizing pulse is excluded. Table 6(D) shows the variation in the

level of the background noise produced by excluding the leading and trailing edges of the pulse. With the leading edge just omitted, the noise output was about 53 db below the output on 100% modulation, and this value (which was obtained by objective measurement) is in agreement with that obtained during the normal subjective readings of Fig. 12. Table 6 shows that this is an improvement of about 4 db over the figure realized when both edges were included.

From this picture of the operation of the system under impulsive noise, the performance of a specific circuit may be estimated, by making adjustments to, for example, the graph of Fig. 12 to comply with the particular conditions obtaining.

The use of negative modulation would offer the advantage that it would no longer be necessary to delay the gate by  $3 \mu\text{sec}$  in order to obtain the suggested 8-db noise reduction. The noise impulses marked 'A' (Fig. 14) would then lie outside the synchronizing pulse. On the other hand, the possibility of additional noise due to gate shift would be increased, and the relative magnitude of the 'positive' and 'negative' noise impulses would be altered, necessitating some modification of the optimum window position.

The readings also show the advantage to be obtained by applying blanking or gating pulses to the sound channel in this way, rather than to the vision channel<sup>19</sup>.

When a sound signal is superimposed on the vision signal, the two must be separated in the receiver, and this may be done either on an amplitude or on a time basis. If, with a positive-modulation system, it is arranged that the separation shall be done on an amplitude basis the modulated pulse may be made of larger amplitude than the vision signal. The latter will then fail to reach the limiting amplifier in the sound channel, but the interference on the picture signal will reach this level and break through. Interference will then be collected continuously on sound except during the modulated pulse, when the noise may be avoided by suitable window adjustment, although this would now be more difficult. In this arrangement the blanking pulse is applied to the vision circuit in order to prevent the sound signal showing on the picture.

On the other hand if the blanking pulse is used with a suitable gate circuit on the sound channel to separate the sound on a time basis, the noise impulses will be suppressed with the vision signal—except for a very short period of time during each pulse when noise breaks through as explained in connection with the modulated synchronizing-pulse system.

This leads to a very great improvement in the impulsive output signal-to-noise ratio.

#### 4.2 Comparison with Amplitude and Frequency Modulation.

In examining the results, it should be remembered that the transmitter power output was the same throughout the tests on f.m., a.m., (unmodulated carrier) and peak pulse (normal 'black level'). This was considered to be the most convenient condition as there is no universally accepted ratio of vision transmitter power to sound transmitter power, and the results may easily be modified to correspond to any required ratio. In this connection it should be noted that if it is desired to see the effect of such a change, for example on the performance graphs, then whereas the input signal-to-interference ratios may be changed in proportion to the change of signal, the noise output ratios will not necessarily change in a similar manner.

The noise outputs obtained on the three modulation systems are compared in Fig. 12. Attention is again drawn to the fact that the actual performance obtained may deviate from that shown according to the peculiarities of the particular circuit in use. However, the conditions under which the w.m. sync-pulse receiver was operated are stated in the text, and as it is believed that the a.m. and f.m. receivers had no exceptional features, the results relating to them are used here as a guide by which to assess the performance of the system under test.

The graph shows how the levels of the resulting noise outputs sound to the listener, and it will be seen that the w.m. sync system performs most satisfactorily at high input interference levels. When the interference was heavy on both picture and sound, the circuit in use gave about 12 db less noise output than a.m. When the level was such that there was a small amount of noise on the picture, the noise output on sync sound was about equal to that on a.m., and the noise appeared with an input level about 10 db lower than that required on a.m.

The performance obtained on f.m. was superior to that of each of the other two systems, the noise output being less at all input noise levels. It was, however, very important that the receiver should be tuned accurately for minimum noise output before being used, and it was found that with the receiver in use it was impossible to be sure of reaching this condition merely by tuning for minimum distortion in the normal manner. When the receiver was mistuned, the noise appeared to have the character usually associated with a.m. and as the tuning was corrected in the presence of interference the sound changed and

appeared to consist of higher frequency 'clicks' which were not so annoying. A further increase of noise output on f.m., which is not allowed for in Fig. 12, is that occurring when the signal is modulated<sup>14</sup>. This was mentioned in Section 2.3, and proved very noticeable when subjective readings were taken in the presence of audio modulation.

The graphs now make it clear how it was possible to obtain readings (Section 2.3) suggesting that the performance of sync-pulse sound was similar to that of a.m. It will be remembered that approximately equal inputs were required on both systems for equal noise outputs (at some very low noise level). The graph shows that the curves do intersect at some low level, and that (as found before) the input would have to be increased by about 20 db on f.m. to give an equivalent noise output. Further, when the signals were modulated (Section 2.3) so that a larger output noise level was required, the interference input required on a.m. was 28 db larger than that which was sufficient on sync sound. According to Fig. 12 however, the maximum difference in input levels for the same output on these two modulation systems is about 12 db, but in the simple demodulator used in Section 2.3 (Fig. 6) the window was at the tip of the synchronizing pulse. The graph corresponding most nearly to the condition obtaining before is therefore (3) of Fig. 13, and there the maximum difference is about 26 db. Exact agreement would not be expected because of the different bandwidths, window areas, etc., in the two instances, but Fig. 13 clearly substantiates the earlier readings.

The second intersection of the a.m. and w.m. sync graphs (at a higher noise level) was discussed (Section 3.2) in connection with the listening checks which indicated that the graphs do give a true picture of the noise output variations. Mention was also made (Section 3.3) that the r.m.s. value of the output current (or voltage) appears to represent the level as heard by the listener, and that peak readings should not be used. The r.m.s. readings of the noise output levels at the maximum interference input used are given in Table 4 (a.m. and w.m. sync sound), and Table 6 (f.m.).

An interesting paper<sup>22</sup> by Page and Gouriet, published after the completion of these tests, gives the results of field tests dealing with the effect of ignition interference on f.m. In these tests the authors encountered interference fields giving rise to noise outputs ranging from 'imper-

ceptible' to 'very disturbing'—these being rated to be of the order of 50 db apart. This is approximately the range considered in the investigation reported here, and the probability of the occurrence of the various interference levels of Fig. 12 may be estimated from the f.m. readings in Ref. 22, in which the results of individual vehicles were noted and totalled.

## 5 Acknowledgments

The author is indebted to Mr. I. Shoenberg and Mr. G. E. Condliffe, Directors of E.M.I. Research Laboratories Ltd., for permission to publish this summary of the investigation, and for facilities granted in its preparation. He also wishes to thank Mr. H. A. M. Clark for the advice received from him throughout the work.

Valuable assistance in performing the many experimental measurements was received from Mr. R. A. Willard.

## REFERENCES

- British Patent Specification No. 613,857.
- Englesfield, C.C.: "Motor Car Ignition Interference," *Wireless Engineer*, 1946, Vol. 23, p. 265.
- George, R. W.: "Field Strength of Motor Car Ignition between 40 and 450 Mc/s," *Proc. Inst. Radio Engrs*, 1940, Vol. 28, p. 409.
- Howe and Peattie: "An Oscillographic Study of Some Induction Coil Phenomena," *Proc. phys. Soc. London*, 1912, Vol. 24.
- London, V. D.: "A Study of the Characteristics of Noise," *Proc. Inst. Radio Engrs*, 1936, Vol. 24, p. 1514.
- London, V. D.: "The Distribution of Amplitude with Time in Fluctuation Noise," *Proc. Inst. Radio Engrs*, 1941, Vol. 29, p. 50.
- Jansky, K. G.: "An Experimental Investigation into the Characteristics of Certain Types of Noise," *Proc. Inst. Radio Engrs*, 1939, Vol. 27, p. 763.
- Nethercot, W.: "Ignition Interference," *Wireless World*, 1947, Vol. 53, p. 352.
- Pressey, B. G. and Ashwell, G. E.: "Radiation from Car Ignition Systems," *Wireless Engineer*, 1949, Vol. 26, p. 31.
- Gill, A. J. and Whitehead, S.: "Electrical Interference with Radio Reception," *J. Instn elect. Engrs*, 1938, Vol. 83, p. 345.
- Hamburger, G. L.: "Interference Measurement, Effect of Receiver Bandwidth," *Proc. Inst. Radio Engrs*, 1940, Vol. 28, p. 409.
- Tollack, I.: "The Effects of High Pass and Low Pass Filtering on the Intelligibility of Speech in Noise," *J. acoust. Soc. Amer.*, 1948, Vol. 20, p. 259.
- Crosby, M. G.: "Frequency Modulation Noise Characteristics," *Proc. Inst. Radio Engrs*, 1937, Vol. 25, p. 472.
- Smith, D. B. and Bradley, W. E.: "The Theory of Impulse Noise in Ideal Frequency Modulation Receivers," *Proc. Inst. Radio Engrs*, 1946, Vol. 34, p. 743.
- Weighton, D.: "Impulsive Interference in Amplitude Modulation Receivers," *J. Instn elect. Engrs*, 1948, Vol. 95, Part III, p. 69.
- Nicholson, M. G.: "Comparison of Amplitude Modulation and Frequency Modulation," *Wireless Engineer*, 1947, Vol. 24, p. 197.
- Haard, B.: "Signal to Noise Ratios in Pulse Modulation Systems," *Ericsson Technics*, 1948, No. 47.
- Fredendall, G. L., Schlesinger, K. and Schroeder, A. C.: "Transmission of Television Sound on the Picture Carrier," *Proc. Inst. Radio Engrs*, 1946, Vol. 34, p. 49.
- Lawson, D. I., Ford, A. V., and Kharbanda, S. R.: "A Method of Transmitting Sound on the Vision Carrier of a Television System," *J. Instn elect. Engrs*, 1946, Vol. 93, Part III, p. 251.
- Moskowitz, S. and Grieg, D. G.: "Noise Suppression Characteristics of Pulse Time Modulation," *Proc. Inst. Radio Engrs*, 1948, Vol. 36, p. 446.
- Mansford, H. L.: "The Waveform Monitor," *Electronic Engineering*, 1947, Vol. 19, p. 272.
- Page, H. and Gouriet, G. G.: "An Experimental Investigation of Motor Vehicle Ignition Interference," *I.B.C. Quarterly*, October 1948, Vol. 3, p. 182.
- Tibbs, C. E.: "Frequency Modulation Engineering," Chapman and Hall.

# V.F. AMPLIFIER COUPLINGS

## Unsymmetrical $\pi$ -Section Filters

By G. G. Gouriet, A.M.I.E.E.

(Engineering Research Department, B.B.C.)

**SUMMARY**—It is shown that, by a suitable choice of the parameters which define the design of unsymmetrical  $\pi$ -section filters, simple expressions for the performance are obtained, from which the steady-state or the transient response may be calculated. Curves of the amplitude characteristic and the group-delay characteristic are given for various values of the variable parameters, and cases of particular interest are discussed. Finally, the requirements of phase-equalizing networks are given.

### 1. Introduction

THE use of  $\pi$ -section filters as a means of providing efficient intervalve couplings in video-frequency amplifiers has received much attention in recent years. Various authors<sup>1</sup> have suggested that the voltage gain-bandwidth product of a stage employing a simple  $\pi$ -section coupling, in which the stray capacitances of the circuit form the shunt elements, is of the order of 1.5 times as great as is obtained using the two-terminal circuit, commonly known as the shunt-peaking network. More complicated couplings employing a combination of the shunt-peaking circuit and the  $\pi$ -section filter, and providing in addition a greater degree of phase linearity, have also been described<sup>2</sup>, but the disadvantage of such circuits is the critical nature of the adjustments necessary to obtain the optimum performance. A better solution, particularly applicable to the case of multi-stage video amplifiers, is to adopt the simple filter couplings throughout and correct the overall phase characteristic by means of a suitable phase-equalizing network.

The transient response of the various forms of such couplings has also received considerable attention, but in practice the response of a single section is seldom of interest, while to deduce the overall transient response of a number of cascade sections from that of a single section is, in general, a formidable task. Kallman, Spencer and Singer<sup>3</sup> have dealt comprehensively with the transient response of a large number of alternative types of filter and have included the case of cascade stages by means of an artifice, but the filters treated are without phase correction, and the results are of limited application, since with the efficient types of coupling the degree of overshoot is prohibitive when many stages are used.

The purpose of this article is to present design data and generalized performance curves for

various values of termination and varying degrees of asymmetry, so that filters may not only be readily designed to provide a constant amplitude characteristic but may also be chosen to fulfil the purpose of equalizing networks. Curves of the group-delay characteristic are given in each case and data for the design of phase-equalizing sections are included.

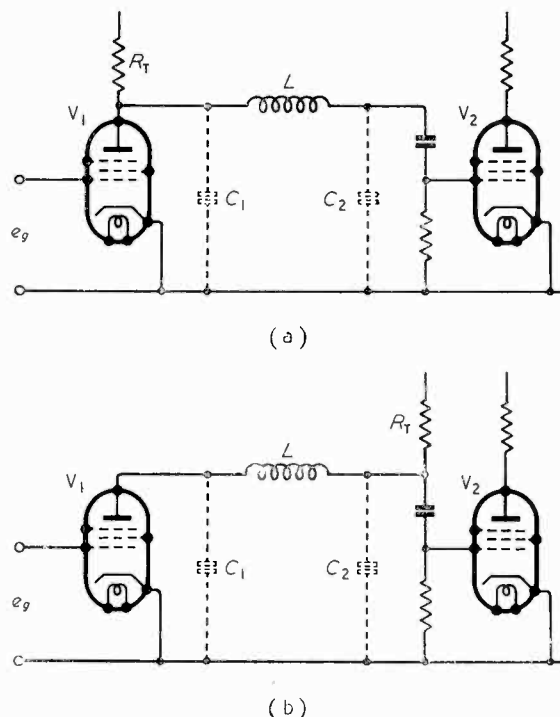


Fig. 1.  $\pi$ -section filters with input termination (a) and output termination (b).

### 2. Design Theory

In this section we shall deal with the design of intervalve couplings of the simple type shown in Fig. 1(a) and (b), and these two cases we shall designate 'input terminated and output term-

MS accepted by the Editor, December 1949

inated' respectively. In general, the valve will be a pentode, having an amplification factor and mutual conductance of  $\mu$  and  $g_m$  respectively, and since we are dealing with wide-band video amplifiers, the value of  $R_T$ , the terminating resistance, will in all cases be very small compared with the valve a.c. resistance,  $r_a$ , and we shall, therefore, justifiably regard the latter as infinite.

The generalized equivalent circuit is shown in Fig. 2,  $e_g$  being the voltage applied to the grid of the valve.

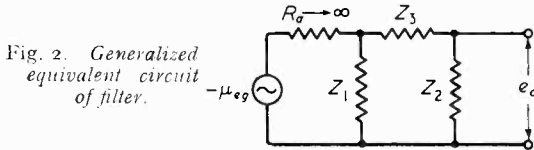


Fig. 2. Generalized equivalent circuit of filter.

For the output voltage,  $e_o$ , we have,

$$e_o = -\mu e_g \frac{Z_1 Z_2}{r_a (Z_1 + Z_2 + Z_3) + Z_1 (Z_2 + Z_3)} \quad (1)$$

Putting  $\mu = g_m r_a$  where  $g_m$  = mutual conductance, and letting  $r_a \rightarrow \infty$  we obtain

$$e_o = -e_g g_m \frac{Z_1 Z_2}{Z_1 + Z_2 + Z_3} \quad (2)$$

Since we are only interested in the characteristic of the transfer impedance  $Z_T$ , we may write more simply:—

$$Z_T = \frac{Z_1 Z_2}{Z_1 + Z_2 + Z_3} \quad (3)$$

A point of fundamental importance to be noted from (3) is that the characteristic of the network is unaltered by the interchange of  $Z_1$  and  $Z_2$ . Thus the networks of Fig. 3(a) and (b) will have identical voltage transfer characteristics, and a generalized analysis is greatly simplified by virtue of this property, as will be shown later.

If the appropriate impedances of the configurations of either Fig. 3(a) or (b) are substituted in (3) we obtain for the normalized voltage transfer factor,  $\theta_T$ , the following expression,

$$\theta_T = \frac{I}{\frac{p^3 L C^2 R_T}{K} + \frac{p^2 L C}{K} + p C R_T (I + \frac{I}{K}) + I} \quad (4)$$

The Heaviside operator  $p$ , has been used in place of  $j\omega$  since this leads to neater algebra and a more general result.

The question now arises as to what parameters can best be introduced in order to express the performance in general terms.

First, let us consider the choice of terminating resistance. In conventional filter theory for a low-pass filter this is chosen to equal the value of the image impedance at zero frequency, and is

termed the design impedance. If, by the standard method, we deduce the image impedances  $Z_{o1}$  and  $Z_{o2}$  for the unsymmetrical filter, we obtain at zero frequency

$$Z_{o1} = Z_{o2} = \sqrt{\frac{K}{I + K}} \sqrt{\frac{L}{C}} \quad (5)$$

This value may be defined as  $\sqrt{(L/C_0)}$  where  $C_0$  is the sum of the two capacitances  $C$  and  $C/K$ , which is in agreement with the symmetrical theory when  $K = I$ .

Bearing in mind the asymmetry, intuitively, we should not expect the most suitable design impedance to be the same for the alternative terminations. Guided by the principles of impedance transformation, let us regard this as a geometric mean value, and use a value of terminating resistance which is equal to the image impedance at zero frequency modified by a factor equal to the ratio of the terminating reactance and the geometric mean of the two reactances. Designating the input and output terminating resistances as  $R_{T1}$  and  $R_{T2}$  respectively, we will obtain,

$$R_{T1} = \sqrt{\frac{K}{I + K}} \cdot \sqrt{\frac{L}{C}} \cdot \frac{X_c}{\sqrt{K X_c^2}} = \frac{I}{\sqrt{I + K}} \cdot \sqrt{\frac{L}{C}} \quad (6)$$

$$R_{T2} = \sqrt{\frac{K}{I + K}} \cdot \sqrt{\frac{L}{C}} \cdot \frac{K X_c}{\sqrt{K X_c^2}} = \frac{K}{\sqrt{I + K}} \cdot \sqrt{\frac{L}{C}} \quad (7)$$

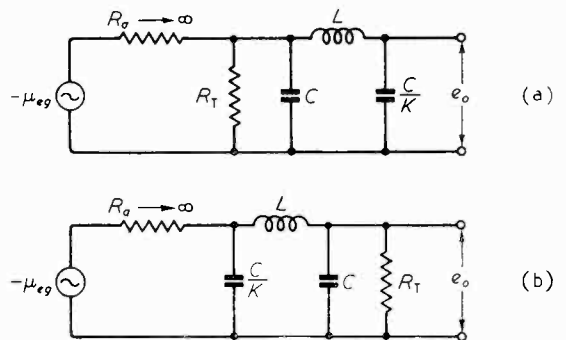


Fig. 3. Circuits (a) and (b) have identical response characteristics.

Under these conditions the input-terminated filter will be as shown in Fig. 4(a), while the output-terminated case will be as in Fig. 4(b). The latter has been shown by (3) to be equivalent to the configuration of Fig. 4(c) and by making substitutions

$$\frac{C}{K} = C' \text{ and } K = \frac{I}{k}$$

we obtain the configuration of Fig. 4(d). This will be seen to be identical with that of Fig. 4(a), except that the reciprocal value of  $K$  has been substituted.

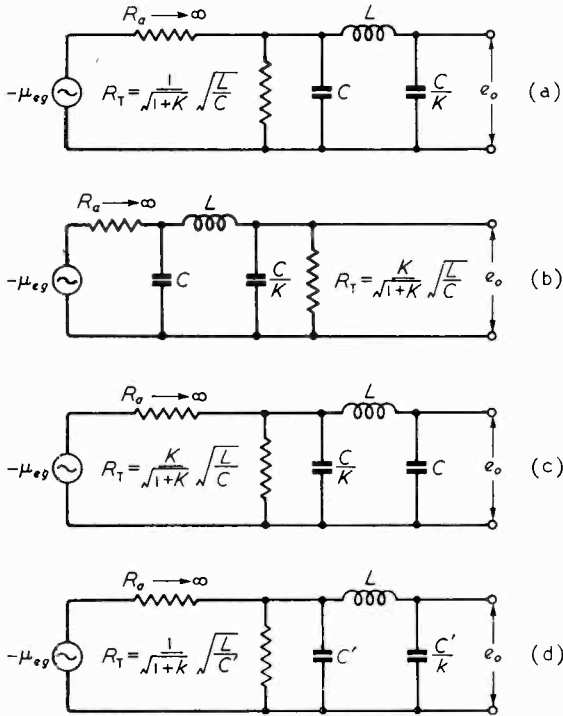


Fig. 4. Input- and output-termination filters are shown at (a) and (b) with the proper component relations. Equivalent filters are (c) and (d).

Again, to follow conventional filter theory let us define the design frequency\* to be that of the loop resonance, i.e., by

$$\omega_0 L - \frac{1}{\omega_0 C} - \frac{K}{\omega_0 C} = 0 \text{ where } \omega_0 = 2\pi \times \text{design frequency} \quad \dots (8)$$

whence  $\omega_0^2 = \frac{1+K}{LC} \quad \dots (9)$

As before, making the substitutions

$$\frac{C}{K} = C'; \quad K = \frac{1}{k}$$

we get  $\omega_0^2 = \frac{1 + \frac{1}{k}}{L \cdot \frac{C'}{k}} = \frac{1+k}{LC'} \quad \dots (10)$

which is again of identical form to (9), except that the value of  $k$  is reciprocal.

Thus we need only examine the case of an input termination, since the corresponding output

termination will simply modify the performance characteristic in the same manner as if the value of capacitance ratio had been reciprocal.

In the foregoing we have chosen to define the design frequency by the relationship

$$\omega_0^2 = \frac{1+K}{LC} \quad \dots (9)$$

and the terminating resistances as

$$R_{T1} = \sqrt{\frac{1}{1+K}} \sqrt{\frac{L}{C}} \text{ for input termination} \quad \dots (6)$$

and  $R_{T2} = \sqrt{\frac{K}{1+L}} \sqrt{\frac{L}{C}} \text{ for output termination} \quad \dots (7)$

By combining (9) with (6) and (7) we may rewrite the latter equations as

$$R_{T1} = 1/\omega_0 C \quad \dots (11)$$

$$R_{T2} = K/\omega_0 C \quad \dots (12)$$

Substituting these values for  $R_T$  in (4) and also using (9) we obtain, for the transfer factor,  $\theta_{T1}$ , corresponding to the case of input termination,

$$\theta_{T1} = \frac{K}{\left(\frac{\phi}{\omega_0}\right)^3 + \left(\frac{\phi}{\omega_0}\right)^2 + \frac{\phi}{\omega_0} + \frac{K}{1+K}} \quad \dots (13)$$

and for  $\theta_{T2}$ , corresponding to output termination,

$$\theta_{T2} = \frac{1}{\left(\frac{\phi}{\omega_0}\right)^3 + \left(\frac{\phi}{\omega_0}\right)^2 + \frac{\phi}{\omega_0} + \frac{1}{1+K}} \quad \dots (14)$$

which factors are identical if  $1/K$  is substituted for  $K$  in one of them. The simplicity and symmetry of these expressions would indicate that our choice of parameters has been the most suitable.

The transfer factors as expressed in (13) and (14) are in suitable form for direct insertion into the Heaviside expansion theorem, from which the transient response may be deduced. However, the labour involved is formidable and bearing in mind the limited value of this knowledge as has been already discussed, we shall be concerned only with the steady-state response.

Substituting  $j\omega$  for  $\phi$  in (13), and using polar co-ordinates, we obtain

$$|\theta_{T1}| / \phi = \frac{K}{\sqrt{A^2 + B^2}} \left/ \tan^{-1} \frac{B}{A} \right. \quad \dots (15)$$

where  $A = \frac{1+K}{K} - \left(\frac{\omega}{\omega_0}\right)^2$

$$B = \left(\frac{\omega}{\omega_0}\right) - \left(\frac{\omega}{\omega_0}\right)^3$$

For the group delay, we have by definition

$$\tau = \frac{d\phi}{d\omega} = \frac{d(\omega/\omega_0)}{d\omega} \cdot \frac{d\phi}{d(\omega/\omega_0)} = \frac{1}{\omega_0} \cdot \frac{d\phi}{d(\omega/\omega_0)}$$

A convenient factor for plotting is thus the normalized delay

$$\omega_0\tau = \frac{d\phi}{d(\omega/\omega_0)}$$

From (15), by differentiation, we obtain,

$$\frac{d\phi}{d(\omega/\omega_0)} = \omega_0\tau = -\frac{\left(\frac{\omega}{\omega_0}\right)^2 \cdot \left[\frac{1-K}{1+K}\right] + \frac{K}{1+K}}{A^2 + B^2} \quad (16)$$

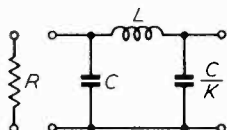
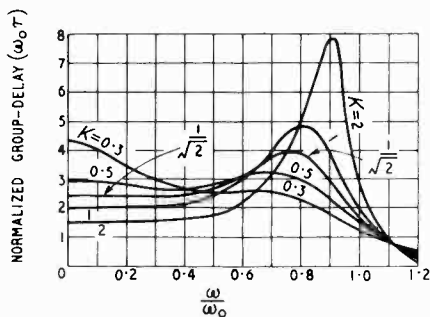
we may vary  $\alpha$  and thus make the termination depart from the design resistance by any amount we please. Making this substitution in (4) we see that  $\alpha$  merely becomes an additional coefficient in the terms containing odd powers of  $\beta$ , whence (15) and (16) become

$$|\theta_{T1}| \angle \phi = \frac{K}{\sqrt{A^2 + \alpha^2 B^2}} \left/ \tan^{-1} \alpha \frac{B}{A} \right. \quad (18)$$

$$\omega_0\tau = -\alpha \frac{\left(\frac{\omega}{\omega_0}\right)^2 \cdot \frac{1-K}{1+K} + \frac{K}{1+K}}{A^2 + \alpha^2 B^2} \quad (19)$$

The effect of varying the value of  $\alpha$  over small limits is shown in Figs. 6, 7 and 8 for the cases of  $K = 0.5, 1.0$  and  $2.0$  respectively.

A case of particular interest is that of  $K = 0.5; \alpha = 0.85$ .

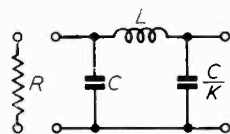
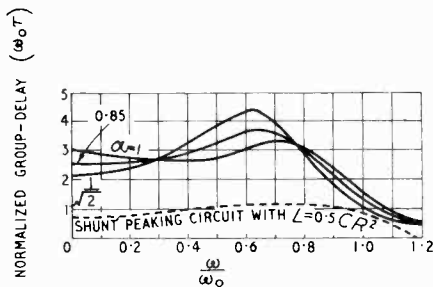
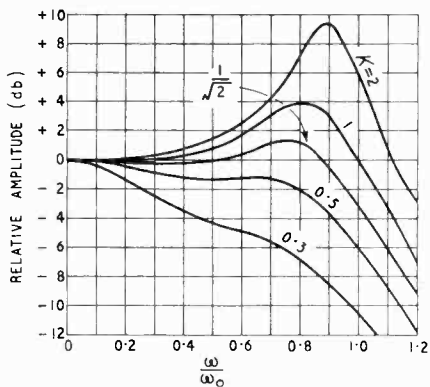


$$R = \frac{1}{\sqrt{1+K}} \sqrt{\frac{L}{C}}$$

Fig. 5. (left) Amplitude and group-delay characteristics for various values of K.

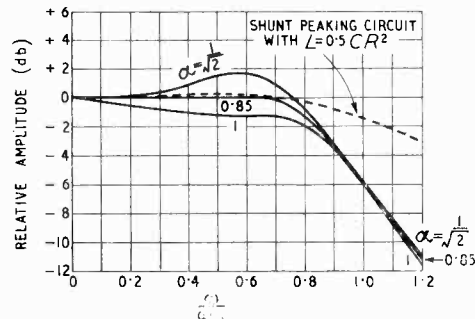
FOR OUTPUT TERMINATION  
PUT  $R = \frac{K}{\sqrt{1+K}} \sqrt{\frac{L}{C}}$  AND  
USE CURVE OF VALUE  $\frac{1}{K}$

Fig. 6. (below) Amplitude and group-delay characteristics with change of  $\alpha$  for  $K = 0.5$ .



$$R = \frac{\alpha}{\sqrt{1+K}} \sqrt{\frac{L}{C}}$$

FOR OUTPUT TERMINATION  
PUT  $R = \frac{\alpha K}{\sqrt{1+K}} \sqrt{\frac{L}{C}}$  AND  
USE CURVE OF VALUE  $\frac{1}{K}$



Curves of equations (15) and (16) have been plotted (the former in decibels) in Fig. 5 respectively for various values of K ranging from 0.3 to 2.0.

As has already been pointed out, the corresponding curves for the case of output termination are obtained simply by choosing reciprocal values of K. Before commenting upon these results, there is yet another parameter which may usefully be varied.

If we express the values of the input termination resistance as

$$R_T = \sqrt{\frac{\alpha}{1+K}} \sqrt{\frac{L}{C}} \quad (17)$$

This will be seen from Fig. 6 to give an amplitude response which is substantially flat up to a frequency of 0.7 of the design frequency. The corresponding group-delay characteristic over this range does not depart from a constant by

more than approximately  $1/2\pi$  times the period of one cycle of the design frequency, which is equivalent to  $0.7/2\pi$  or approximately 11% of the period of one cycle of the highest operating

network is approximately constant and numerically equal to the value of  $R$  up to the upper angular-frequency limit  $\omega_c$ , at which limit it is also equal to the value of the stray reactance  $1/\omega_c C_s$ . The amplitude and group-delay characteristics are shown by the dotted curves in Fig. 6, in which  $\omega_0$  is  $2\pi$  times the resonance frequency of  $L$  and  $C_s$ .

Since the voltage gain is directly proportional to the value of the load resistance, we have, for similar values of stray capacitance and equal frequency bands, in the case of the shunt-peaking circuit

$$\text{Gain (S.P.)} \propto \frac{I}{\omega_c C [1 + I/K]}$$

and for the filter

$$\text{Gain (F)} \propto \frac{0.7\alpha}{\omega_c C}$$

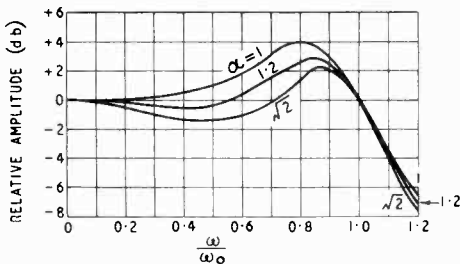
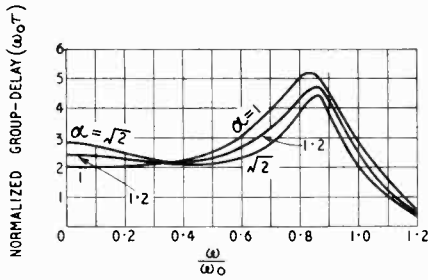
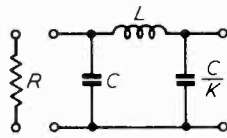


Fig. 7. (above) Amplitude and group-delay characteristics with change of  $\alpha$  for  $K = 1$ .

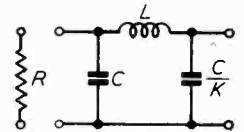
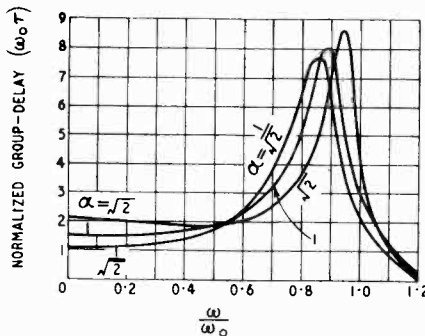
Fig. 8. (right) Amplitude and group-delay characteristics with change of  $\alpha$  for  $K = 2$ .



$$\omega_0 = \sqrt{\frac{1+K}{LC}}$$

$$R = \frac{\alpha}{\sqrt{1+K}} \sqrt{\frac{L}{C}}$$

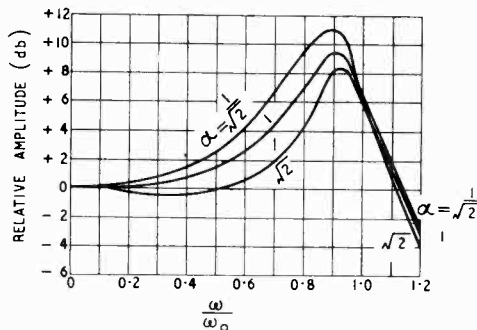
FOR OUTPUT TERMINATION  
PUT  $R = \frac{\alpha K}{\sqrt{1+K}} \sqrt{\frac{L}{C}}$  AND  
USE CURVE OF VALUE  $\frac{1}{K}$



$$\omega_0 = \sqrt{\frac{1+K}{LC}}$$

$$R = \frac{\alpha K}{\sqrt{1+K}} \sqrt{\frac{L}{C}}$$

FOR OUTPUT TERMINATION  
PUT  $R = \frac{\alpha K}{\sqrt{1+K}} \sqrt{\frac{L}{C}}$  AND  
USE CURVE OF VALUE  $\frac{1}{K}$



frequency. Under these conditions, the distortion produced by a single section of the network when accepting waveforms having a spectrum thus restricted will be negligible. The implication of this statement will be discussed in Section 3, which deals with phase correction.

It is interesting to compare the voltage gain of a stage employing this form of coupling with that obtainable from the simple two-terminal network or shunt-peaking circuit shown in Fig. 9 in which  $C_s$  represents the total inter-stage stray capacitance. One form of the shunt-peaking circuit which is often used as a basis for comparison<sup>1</sup>, and which was described in early literature<sup>5</sup>, is obtained by making

$$R = 1/\omega_c C_s = 2\omega_c L$$

where  $\omega_c$  defines the upper-frequency limit of the working frequency band. This relationship may also be expressed by the equations

whence the ratio

$$\frac{\text{Gain (F)}}{\text{Gain (S.P.)}} = 0.7\alpha \left[ 1 + \frac{1}{K} \right]$$

= approx. 1.8 for  $K = 0.5$  and  $\alpha = 0.85$

In a multi-stage amplifier, this gain, which amounts to 5 db per stage, is well worth having,

particularly at the wider bandwidths for which the gain per stage is severely limited.

It will be noted that this particular result is restricted in the case of the filter to circuits for which the total stray capacitance involved can be split up into two capacitances with a ratio of

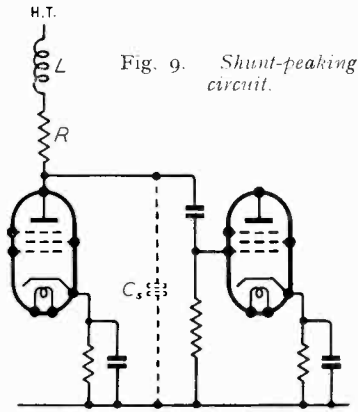


Fig. 9. Shunt-peaking circuit.

2:1, but it is immaterial which of the two capacitances is the larger, since if it is the input capacitance an output termination will provide the same characteristic. In a practical case it may be necessary to add a trimming capacitance to the larger of the two to fulfil this condition and the full advantage of 5 db will not be realized. However, in practice, using modern valves, it is usual for the valve input capacitance to be of the order of twice the valve output capacitance and an approximate 'trim' may often be accomplished by choosing the most suitable position for the grid coupling capacitor, as shown in Fig. 10(a) and (b). On the other hand, when coupling the output of a power valve to the grid or cathode of a c.r. tube for modulation purposes, it is common to find that the valve output capacitance, with associated strays, is of the order of twice the c.r. tube input capacitance, and in this case the desired characteristic is obtained with an input termination.

Another response curve of interest is the case of  $K = 1, \alpha = 1$ . (Fig. 7). This is simply the case of the 'constant- $k$ ' symmetrical filter, and the response, which rises slowly to a maximum of +4.0 db at approximately 0.8 of the cut-off frequency, is useful for providing a small amount of 'top-lift' to compensate for other deficiencies; for example, aperture distortion. Larger degrees of high-frequency correction may be obtained by using a value  $K = 2$ , and values of  $\alpha < 1.0$ .

### 3. Phase Correction

#### 3.1 Practical Considerations

Undoubtedly the most important present day application of video-frequency amplifiers is in

the provision of amplification for television signals, and in this section we shall base our discussion in terms of such signals, and concentrate particular attention on the unit-step waveform, which in television corresponds to the sudden transition from a black to a white area or vice versa.

T. C. Nuttall has already made a comprehensive study of phase equalization, and a paper by him dealing with this subject was presented at Zurich, in September 1948<sup>4</sup>. We shall review the question here, briefly, since it has considerable bearing on the choice of interval couplings.

In the previous section it was shown that the characteristic of a coupling filter which has the parameters  $K = 0.5$  and  $\alpha = 0.85$  (see Fig. 7) is such that a signal will be transmitted through the filter with negligible distortion, provided the spectrum of the signal is limited to a maximum frequency,  $\omega_c$ , equal to 0.7 of the design frequency,  $\omega_0$ . If, however, a unit-step signal, obtained, for example, from an ideal camera, is applied to the filter without any modification to its spectrum, the output we should obtain would be of the form

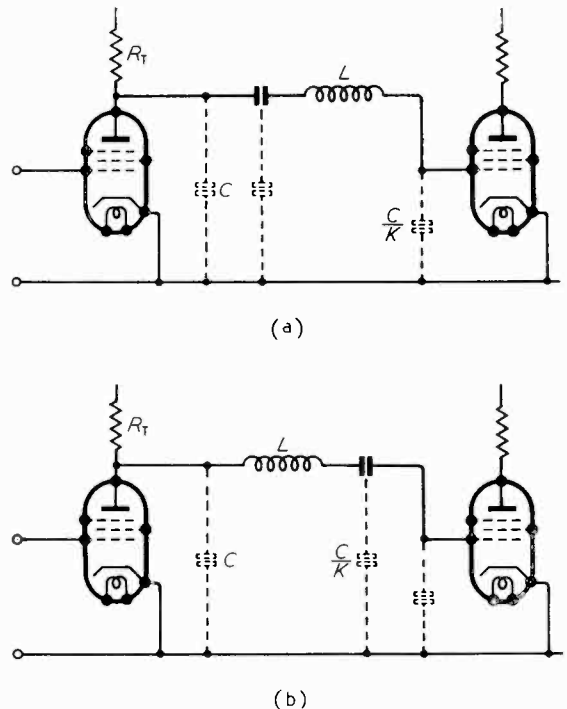


Fig. 10. Shows how position of grid-coupling capacitor may be chosen to assist 'trimming.'

shown in Fig. 11(a), and if several stages employing similar couplings were used in cascade due to the increased rate of cut-off and the more rapid departure from a linear phase characteristic

near the cut-off frequency, the output waveform would be even more distorted and of the form shown in Fig. 11(b). Such response waveforms would, of course, only be acceptable for television, in cases where the cut-off frequency,  $\omega_c$ , was arranged to be greater than the frequency corresponding to the limiting optical resolution of the reproducing system. In other words, if the pattern produced by the distortion could not be resolved by the reproducing screen, then the distortion would be of no consequence.

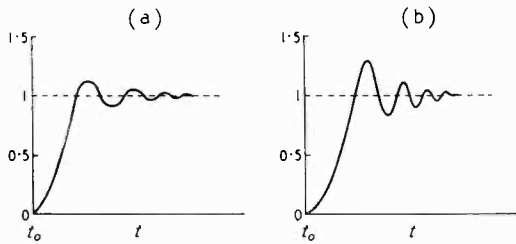


Fig. 11. Response of single filter to unit-step input (a), and response of cascade filters (b).

It is also true that if the television camera were incapable of resolving the form of a similar pattern, due, for example, to optical or electro-optical limitations, the distortion caused by the filter would be relatively insignificant. By definition, the spectrum of the signal applied to the filter would then be confined substantially to within the cut-off limit of the filter.

This is in effect saying that it is not permissible to introduce a sharp cut accompanied by phase distortion into the video characteristic except at a frequency higher than that which corresponds to the finest detail which the electro-optical elements of the system can resolve.

Let us consider what this means in terms of a 405-line system of television. If detail corresponding to 405 lines in the horizontal direction is to be reproduced without severe loss of contrast ratio, a video-frequency characteristic is required which is substantially flat up to a limit of approximately 3.0 Mc/s. Since it is not permissible to introduce a sharp cut at this limiting frequency by means of straightforward filters, the complete electrical system should be designed to have a considerably wider bandwidth than this, say 5 Mc/s, whether a sharp cut-off or a trailing characteristic is used, and, remembering that in practice the electrical system includes the complete transmitting and receiving apparatus, the requirement is most uneconomical.

As an alternative it might be argued that the whole of the electrical system following the camera tube could be designed to have a cut-off frequency of a little over 3.0 Mc/s, and that cut-

off distortion could be avoided by confining the spectrum of the camera output signal to within this limit. Since, however, we require that the response from the camera should be substantially unattenuated at 3.0 Mc/s, this could only be achieved by means of a filter with a very sharp cut-off, which would of course result in the very distortion we are endeavouring to avoid. On the other hand, to limit the spectrum of the camera output signal by means of a gradual cut-off implies that the attenuation must commence at a relatively low frequency, say 1.0 Mc/s, and increase steadily up to the limiting frequency of 3.0 Mc/s, the result of which will be to cause a considerable deterioration in definition.

All this is true when the electrical characteristic is determined by means of conventional filters without phase correction. If, however, a phase equalising network is introduced into the electrical system, so that at the output of the system all components over the pass band arrive with a constant delay (i.e., the overall phase characteristic is linear), a different state of affairs will exist.

Clearly in such circumstances any symmetrical function, whether odd or even, will remain a symmetrical function since only the amplitudes of the components of its spectrum will have been modified, and in the limit for an infinitely sharp cut-off, the waveform resulting from a unit-step input will be of the form shown in Fig. 12. It is a simple matter to show that the resulting time function is in this case the sine-integral function for which the over-shoot is less than 10%, an amount which is scarcely perceptible when viewed on a television screen. For any slower

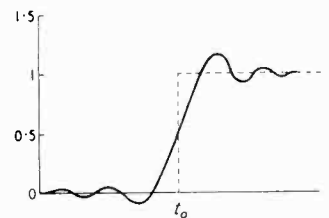


Fig. 12. Response to unit-step input of a phase-equalized filter.

rate of cut-off, the overshoot will be less than this, and the waveform of Fig. 12 is therefore representative of the worst case.

It will be noted from Fig. 12 that the arrival of the 'step' is anticipated by ripples which appear in the waveform prior to the time,  $t_0$ , at which the step actually occurs. This does not, of course, imply that the ripples occur before the step has been applied to the filter, but simply that the phase-equalising network must necessarily introduce a time delay in order to produce the desired effect of advancing the arrival time of the high-frequency components relative to that of the low frequencies.

To obtain precise phase-equalization of any practical filter would require an infinite number of sections in the equalizing network, and the delay through the equalizer would thus be infinite. This is obviously true, since if the output waveform due to unit step input is to possess perfect odd symmetry, the ripples must commence at a time  $-\infty$  relative to the actual step and an infinite delay is thus a necessary postulate.

constant-resistance lattice structure, as shown in Fig. 13(a). The parameters of such a section may be defined as follows:

$$L = \frac{R_0}{\beta \omega_0} ; C = \frac{1}{\beta \omega_0 R_0}$$

where  $L, C$  and  $R_0$  are as shown in Fig. 13(a) and  $\beta$  is a design constant which determines the equalizing characteristic.

We thus have,

$$R_0^2 = \frac{L}{C} ; \text{ and } \omega_0^2 = \frac{1}{\beta^2 L C}$$

Since the network has an all-pass characteristic the only significance of  $\omega_0$  is that it is a design frequency which will determine the range over which a given phase characteristic will be obtained.

For a given termination and design frequency the only variable parameter is  $\beta$  and the transfer constant may be expressed as

$$\theta = 1.0 / 2 \tan^{-1} \beta \left[ \frac{\omega}{\omega_0} - \frac{\omega_0}{\omega} \right]$$

Differentiating the argument with respect to  $\omega$

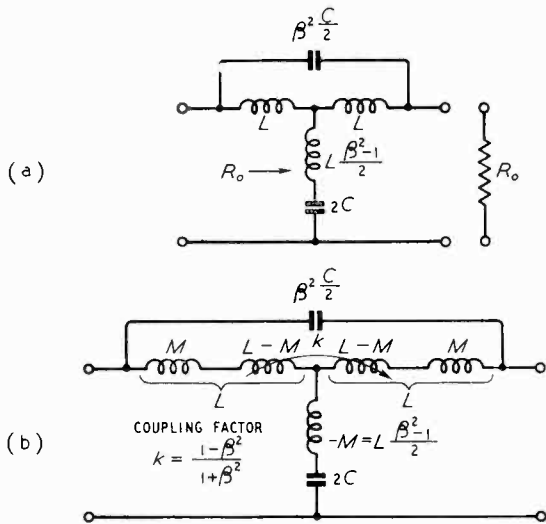
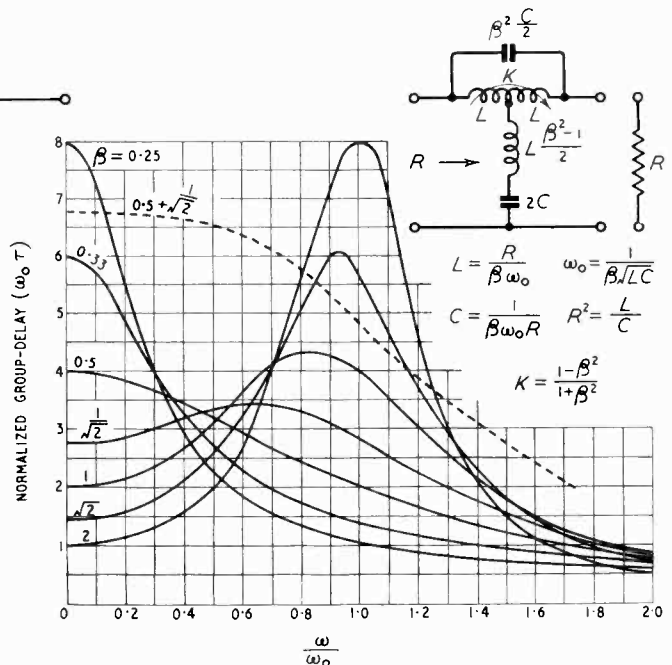


Fig. 13. (above) Phase-equalizing circuit (a) and the arrangement to be adopted (b) when the shunt inductance is required to be negative.

Fig. 14. (right) Group delay-characteristic of phase equalizer.



In practice, a delay equal to the period of two or three cycles of the cut-off frequency is sufficient to provide substantial symmetry and an equalizer having four sections is usually adequate.

By means of phase-equalization it is, therefore, possible to obtain a transient response which is satisfactory for television purposes, even though the cut-off frequency of the electrical system is chosen to equal the frequency which corresponds with the finest detail which it is required to resolve.

### 3.2 Design of Phase-Equalizing Sections

A most convenient form of phase-equalizing section is the bridged-T equivalent of the all-pass

we obtain for the normalized group delay

$$\omega_0 \tau = \frac{2\beta \left[ 1 + \left( \frac{\omega}{\omega_0} \right)^2 \right]}{\beta^2 \left[ 1 - \left( \frac{\omega}{\omega_0} \right)^2 \right]^2 + \left( \frac{\omega}{\omega_0} \right)^2}$$

Curves of this expression are given in Fig. 14

for values of  $\beta$  ranging from  $\beta = 0.3$  to  $\beta = 4.0$ .

It will be noted that for values of  $\beta < 1.0$  the inductance in the shunt element is negative and is therefore provided by mutual coupling between the two inductances in the series element, as shown in Fig. 13(b). If the coupling factor,  $k$ , is expressed in terms of  $\beta$  we obtain

$$k = \frac{1 - \beta^2}{1 + \beta^2}$$

The process of designing a phase equalizer for correcting a given filter characteristic is unavoidably tedious. Assuming that the group-delay characteristic of the filter is known, the simplest method is to 'combine' various equalizing characteristics by trial and error, using the curves of Fig. 14, until a satisfactory compensating characteristic is obtained. By a suitable choice of  $\omega_0$ , the working range of each section may be made to coincide with any desired frequency band, and for a complete equalizer the value of  $\omega_0$  is not necessarily the same for all sections.

A useful combination which may be used as a basis for equalizing most forms of filter is two sections comprising

$$\text{one } \beta = \frac{1}{2} \text{ and one } \beta = \sqrt{\frac{1}{2}}$$

The combined characteristic is shown dotted in Fig. 14, and will be seen to provide a delay in the arrival time of frequency components which is at first gradually and then rapidly reduced as the frequency is increased.

## Conclusions

A systematic approach to the design of simple  $\pi$ -section intervalve coupling filters has been described and the general question of phase-equalization has been discussed. It is considered that video-frequency amplifiers involving many stages may be designed most efficiently and simply by using these filters throughout and applying overall phase correction by means of a phase-equalizing filter.

## Acknowledgment

The writer wishes to thank the Chief Engineer of the British Broadcasting Corporation for granting permission to publish this article, Mr. H. L. Kirke, C.B.E., M.I.E.E., under whose direction the work has carried out, and also Mr. T. C. Nuttall, of Cinema-Television, Limited, for helpful discussions.

## REFERENCES

- 1 "Principles of Television Engineering," by D. G. Fink, Chapter VI, Sect. 34, pp. 226-227. McGraw-Hill.
- 2 "Radio Engineer's Handbook" F. E. Terman, Sec. 5, Par. 16. McGraw-Hill.
- 3 "Wide Band Amplifier for Television," by H. A. Wheeler, *Proc. Inst. Radio Engrs.* July 1939, pp. 429-438.
- 4 "Transient Response," by Kallman, Spencer and Singer, *Proc. Inst. Radio Engrs.* March 1945, pp. 169-195.
- 5 "Some Aspects of Television Circuit Technique: Phase Correction and Gamma Correction," by T. C. Nuttall, *Bulletin Ass. Suisse Electr.*, Vol. 40, 1949, No. 17, pp. 615-622.
- 6 "L.F. Amplification in Television Receivers," by W. T. Cocking, *Wireless World*, April 26th, 1935, p. 417.

# NARROW-PULSE GENERATOR

*For Calibrating Noise-Measuring Sets*

By C. S. Fowler, A.M.Brit.I.R.E.

(Communication from the National Physical Laboratory)

## 1. Introduction

This paper describes the design of a generator of pulses of known amplitude and known repetition rate, the latter being adjustable so as to provide either single pulses, or recurrent pulses having a repetition frequency between 5 and 5,000 pulses per second, and the shape of the pulses being such as to give an energy spectrum flat within 0.2 db up to 30 Mc/s and only 1 db down at 40 Mc/s.

Such a generator is required for the calibration of radio noise-measuring sets. It is also useful

for the study of the frequency characteristics of radio receivers and of networks generally.

## 2. Pulse-Forming Circuit

The pulse-forming circuit is similar to one developed by the U.S. Signal Corps,<sup>1</sup> and is shown in Fig. 1.

The pulses are produced by the discharge of the capacitor  $C$  through  $R_1$  and the thyatron  $V_1$ , the fall of potential at  $P$  is then differentiated in the network  $C_1R_A$ , (where  $R_A$  is the effective resistance between  $X$  and earth of the portion of the circuit to the right of  $AA$ ) to form the output pulse.

MS accepted by the Editor, January 1950.

The thyatron used is the miniature 2D21—a Xenon-filled tetrode capable of passing 500 mA peak cathode current, with an ionization time of between 0.05 and 1  $\mu$ sec and a normal de-ionization time of 130  $\mu$ sec. The ionization time falls with increasing triggering voltage and is

shown in Fig. 2. It consists of a blocking oscillator driving a cathode-coupled multivibrator.

The frequency of the wide-range blocking oscillator<sup>3</sup> is controlled by the 5-M $\Omega$  potential divider (Section A, Fig. 2), and, with the nominal values of components shown, covers 5 to 5,300 c/s.

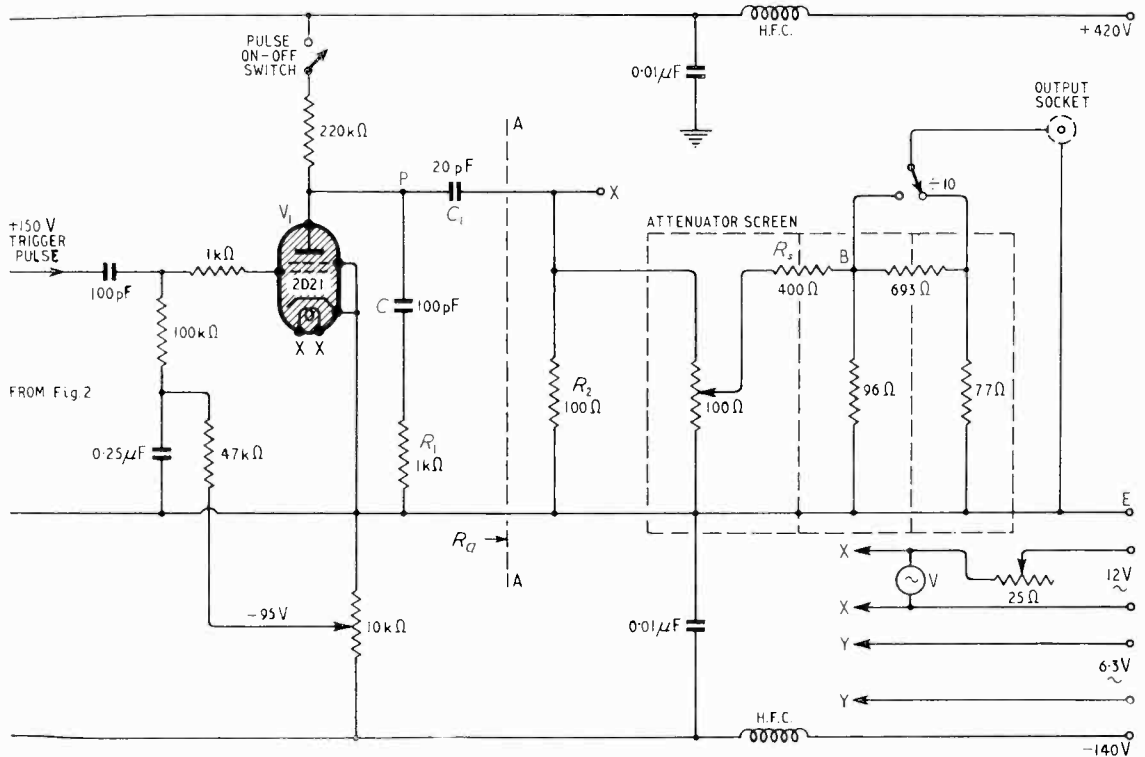


Fig. 1. Pulse-forming circuit and attenuator.

approximately 0.3  $\mu$ sec for a pulse of some 60-volts amplitude.

The de-ionization time can be reduced by holding the grid highly negative between triggering pulses. With a holding potential of some 95 volts repetition frequencies of the order of 7,000 c/s have been obtained without erratic operation of the thyatron.

The shape of the output pulse and its amplitude are dependent on the inductance of the leads forming the output network and on the stray capacitances between point X, Fig. 1, and earth.

In order to minimize these effects the thyatron is mounted on a sub-chassis immediately over the output attenuator network, capacitor C<sub>1</sub> forming the lead through the chassis between the thyatron anode pin and R<sub>2</sub>, as shown in Fig. 5.

### 3. Triggering Circuit

The circuit used to generate the required repetition frequency, and to trigger the thyatron,

The blocking-oscillator frequency is critically dependent on the h.t. and bias voltages, as is the amplitude of the pulse generated by the thyatron, making regulated supplies essential. Two 280/40 stabilovolts connected in series were used in the original power pack, with the earth connection arranged to give 420 volts positive and 140 volts negative, the total current consumption being 22 mA.

The waveform of the pulses from the blocking oscillator is not suitable for directly triggering the thyatron, the triggering pulse for which is obtained from the cathode resistor of the multivibrator (Section B, Fig. 2) which in turn is triggered by negative pulses obtained from the blocking-oscillator anode.

The pulse produced by the multivibrator has an amplitude of approximately 150 volts positive and a duration of some 20  $\mu$ sec. This is differentiated before application to the thyatron lead.

The amplitude of the thyatron output pulse

was found to be somewhat dependent on the triggering pulse amplitude especially at the higher frequencies. To avoid this effect a compensating inductance is used in the multivibrator circuit, which is otherwise of normal construction.

Single pulses are obtained by switching off the blocking oscillator to prevent possible break through, and applying negative pulses by means of a push switch.

#### 4. Performance

##### 4.1 Theory

It is convenient to describe the amplitude of a pulse in terms of the equivalent sine-wave voltage. This is the sine-wave voltage which has an amplitude equal to the peak amplitude of the pulse as observed in the particular network under consideration.

For a pulse derived from the discharge of a capacitor through a resistor, it can be shown (see Appendix) that the equivalent r.m.s. sine-wave voltage is given approximately by:

$$E = \sqrt{2} V_0 RC \Delta f \dots \dots \dots (1)$$

where

- $E$  = equivalent r.m.s. sine-wave voltage,
- $V_0$  = voltage to which the capacitor is charged,
- $C$  = capacitance (farads),
- $R$  = discharge resistance (ohms),
- $\Delta f$  = bandwidth in c/s of circuit in which voltage is developed.

For the circuit shown in Fig. 1

- $E = \sqrt{2} V_0 R_A C_1 \Delta f / K_1 \times 10^6 \dots \dots (2)$
- $E$  = equivalent r.m.s. sine wave in microvolts at B with the variable attenuator set at full output,
- $V_0$  = h.t. voltage less thyatron drop,
- $R_A$  = resistance of input to the attenuator network at A A'
- $\Delta f$  = bandwidth in c/s,
- $R_B$  = resistance between B and earth of the circuit to right of B,
- $R_s$  = series resistance,
- $K_1 = R_B / (R_s + R_B)$ .

Inserting in (2) the measured values  $V_0 = (420 - 10)$ ,  $R_A = 45.5 \Omega$ ,  $C = 24 \times 10^{-12} F$ ,  $\Delta f = 1,000$  c/s,  $R_B = 85 \Omega$ ,  $R_s = 400 \Omega$ ,  $K_1 = 0.175$ ,  $E = 110 \mu V$  r.m.s. at B

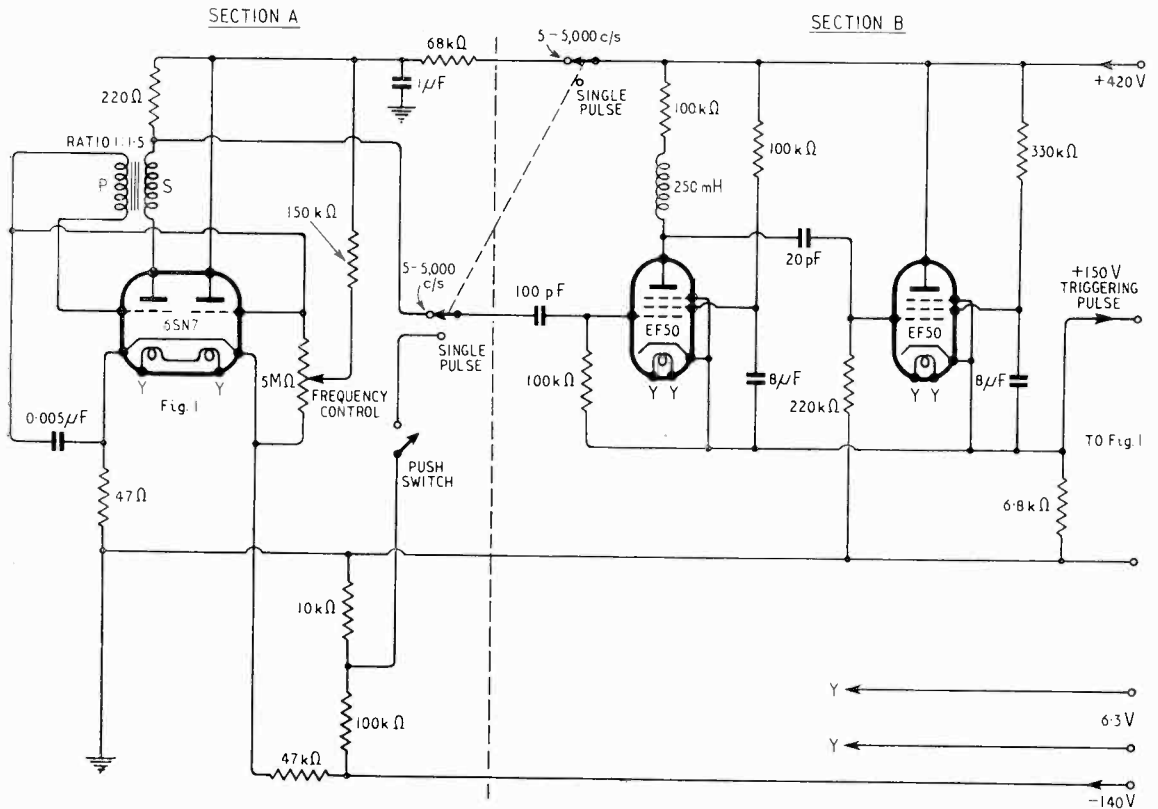


Fig. 2. Variable frequency triggering voltage generator.

A further attenuation factor of 0.005 was introduced between the full output and the voltage applied to the receiver during the measurements, giving theoretically  $0.55 \mu\text{V}$  r.m.s.

#### 4.2 Measurement

The performance of the generator was measured using stabilized h.t. and bias supplies of +420

The pulse repetition rate was kept at 400 c/s throughout the series of measurements. The generator output and receiver attenuators were adjusted so that a suitable output amplitude was obtained without overloading of the receivers occurring at any frequency. The receiver tuning was then set at a specific frequency, the output from the pulse generator applied to the input, and the output amplitude measured on an oscilloscope.

Similar measurements were made on other frequencies between 300 kc/s and 90 Mc/s, the receiver gain being set to the same value each time with the aid of a standard signal generator. The measured relative voltage spectrum is plotted in Fig. 3.

To determine the equivalent sine-wave voltage by measurement, the amplitude versus frequency characteristic of a suitable 2.25-Mc/s amplifier was plotted in the normal manner, and the area under the resulting curve measured, this was divided by the response at the mean

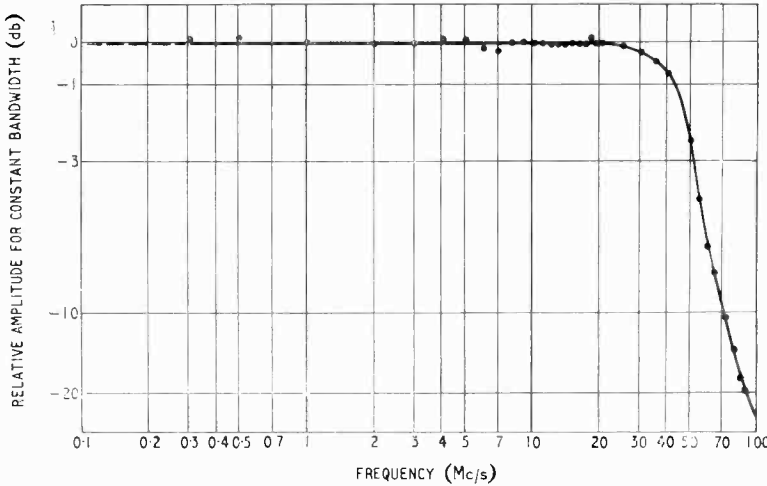
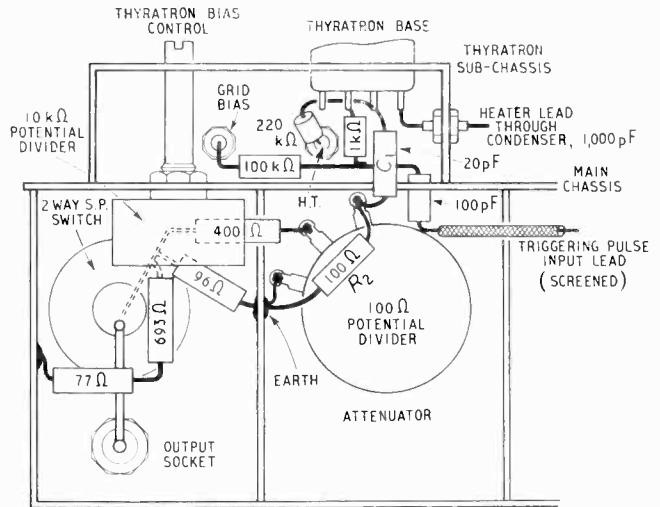
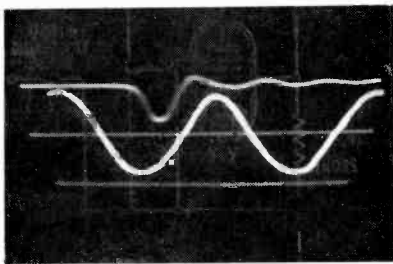


Fig. 3 (above). Pulse generator frequency spectrum.

Fig. 4 (below). Oscillogram of output pulse.

Fig. 5 (right). Thyatron sub-chassis and attenuator compartment. View from rear of panel.



and -140 volts. The thyatron grid bias was set to -95 volts and its heater voltage to 6.8 volts. For measurements of the r.f. spectrum two receivers both having built-in attenuators were used, one covering the range 300 kc/s to 25 Mc/s and the other 15 to 120 Mc/s. The r.f. bandwidths were wider than the i.f. bandwidths to ensure a constant effective bandwidth over all ranges.

frequency to obtain the bandwidth of an equivalent idealized amplifier.

The output of the pulse generator was then applied to the input of the amplifier and the peak amplitude of the pulse as displayed on the oscilloscope noted. A standard signal generator tuned to the mean frequency of the amplifier was then substituted for the pulse generator and its output adjusted to give the same peak amplitude on the oscilloscope as was obtained from the pulse generator. Both inputs were

applied to the amplifier through an attenuating resistive pad to minimize detuning effects on the first circuit.

The results of the above measurements were as follows:—

- Equivalent amplifier bandwidth = 27.5 kc/s
- Sine-wave voltage to give same peak indication as pulse generator corrected for terminating-pad impedance = 20.6  $\mu$ V
- Dividing factor of terminating pad = 10

These figures give a measured value of equivalent sine-wave voltage of 0.75  $\mu$ V per kc/s compared with the theoretical value of 0.55  $\mu$ V per kc/s already derived.

### 5. Conclusions

The shape of the pulse produced by the generator as observed on a particular high-speed oscilloscope is shown in Fig. 4, the timing wave having a frequency of 25 Mc/s and the horizontal lines representing 50- and 100-volt levels measured from the pulse base line.

From this oscillogram the apparent pulse width is 0.01  $\mu$ sec which is some ten times the true pulse length of the discharge time constant. Moreover the amplitude is seen to be 38 volts, which is about one-tenth of the charging voltage  $V_0$ . This indicates that the oscillograph circuit was not capable of indicating the true form of such narrow pulses; i.e., of time duration 0.001  $\mu$ sec.

The approximate theory indicates the order of magnitude of the equivalent sine-wave voltage but, as is seen from the discrepancy between measured and calculated values, it is not apparently sufficiently accurate to enable the instrument to become an absolute standard.

Also as shown in the Appendix the output pulse voltage is independent of the network  $CR_1$  which is only necessary to ensure regular firing of the thyratron, again the exact manner in which the thyratron resistance changes during the discharge time does not enter the calculation as long as  $f \ll 1/RAC_1$ .

### Acknowledgments

The work described above was carried out as part of the programme of the Radio Research Board. This paper is published by permission of the Director of the National Physical Laboratory and the Director of Radio Research of the Department of Scientific and Industrial Research.

The co-operation of the British Electrical and Allied Industries Research Association, in the use of their high-speed oscillograph in order

to obtain the photograph of the pulse, is gratefully acknowledged. The author desires to acknowledge the assistance of R. E. Burgess in connection with the mathematical analysis.

### APPENDIX

*Equivalent sine-wave voltage of a capacitance-resistance discharge voltage*

Let  $E(t)$  be an impulse voltage commencing at  $t = 0$ . Then its frequency spectrum  $F(f)$  is given by the Fourier transform

$$F(f) = \int_0^{\infty} E(t) e^{-j\omega t} dt$$

$$\text{Correspondingly, } E(t) = \int_{-\infty}^{+\infty} F(f) e^{j\omega t} df \quad \omega = 2\pi f$$

Thus in a narrow frequency interval  $\Delta f$  at  $f$  the spectral component of  $E(t)$  can be written as

$$e(t) = [R_e F(f) \cos \omega t + F(-f) e^{-j\omega t}] \Delta f$$

$$= 2 [R_e F(f) \cos \omega t - I_m F(f) \sin \omega t] \Delta f$$

where  $R_e$  and  $I_m$  denote real and imaginary parts. The amplitude of the voltage of frequency  $f$  in a bandwidth  $\Delta f$  is therefore

$$A(f) = 2 |F(f)| \Delta f$$

and the r.m.s. value of the equivalent sine-wave voltage is thus

$$e_{r.m.s.} = \sqrt{2} |F(f)| \Delta f$$

If the impulse is due to a capacitance  $C$  discharging from a voltage  $V_0$  through a resistance  $R$  its time variation is given by

$$E(t) = V_0 e^{-t/RC}$$

whence

$$F(f) = \frac{V_0 RC}{1 + j\omega RC}$$

giving

$$|F(f)| = \frac{V_0 RC}{\sqrt{1 + \omega^2 R^2 C^2}}$$

hence

$$e_{r.m.s.} = \frac{\sqrt{2} V_0 RC \Delta f}{\sqrt{1 + \omega^2 R^2 C^2}}$$

If now  $\omega^2 R^2 C^2 \ll 1$ , the spectrum is flat and given by

$$e_{r.m.s.} = \sqrt{2} V_0 RC \Delta f$$

showing that the equivalent r.m.s. voltage is determined by the area  $V_0 RC$  of the impulse  $E(t)$ . In general when the impulse duration is short compared with  $1/\omega$

$$F(f) = \int_0^{\infty} E(t) dt$$

In the actual circuit under consideration (Fig. 1) the impulse voltage  $E$  is developed across  $R_A$  and its low-frequency spectrum is independent of the network  $CR_1$  and the manner in which the thyratron resistance changes with time. This may be shown as follows:—

$$E = R_A C_1 \frac{dV_{C1}}{dt} \quad \text{where } V_{C1} = \text{voltage across } C_1$$

$$\int_0^{\infty} E dt = R_A C_1 \left[ V_{C1} \right]_0^{\infty} \quad E = \text{voltage across } R_A$$

$$= R_A C_1 V_0 \quad V_0 = \text{charge voltage}$$

whence  $e_{r.m.s.} = \sqrt{2} V_0 R_A C_1 \Delta f$  when  $f \ll 1/R_A C_1$ .

### REFERENCES

- 1 U.S. Signal Corps. "Report RI (U.S.A.) 207" Presented to C.I.S.P.R. Lucerne 1947.
- 2 M. Binbaum. "Measurement of Ionization and Deionization Times of Thyratron Tubes." *Trans. A.I.E.E.*, 1948, Vol. 67, Part 1, pp. 209-214.
- 3 R. Benjamin. "Blocking Oscillators" *J. Instn. elect. Engrs*, 1946, Vol. 93, Part IIIA, pp. 1159-1175.

# CORRESPONDENCE

Letters to the Editor on technical subjects are always welcome. In publishing such communications the Editors do not necessarily endorse any technical or general statements which they may contain.

## Surface Wave Transmission Line

SIR,—Your Editorial in the July number has been read with great interest, and has led to experimental work being carried out upon Surface Wave Transmission. This experimental work reveals clearly that the effect of the dielectric coating is not to improve the transmission properties of the wire in between the launching and collecting horns, as perhaps might be inferred from your Editorial, but to reduce the launching and collecting losses at the horns. This is completely in accord with the curves given in Fig. 4 of the Editorial. These show an increase in transmission losses along the wire as the dielectric thickness is increased, as evidenced by the rising curves marked  $L_i$  and  $L_c$ . The curve  $L_h$  on the other hand, which defines the launching and collecting losses for the particular horns used, falls as the thickness is increased, with the result that the total transmission loss is a minimum with a dielectric coating.

It would seem to be obvious, therefore, that the part played by the dielectric coating is merely to concentrate the electric field near the horns and thus with a given size of horns, to obtain an improved overall effect.

There is sufficient experimental evidence to show that the correct procedure, to obtain minimum losses in any given system, using Surface Wave Transmission, is to use bare wire between the terminal devices, and correctly to design the latter by properly shaping the metal horns, and/or using tapered dielectric loading on the parts of the conductor which come within the field of the horns.

N. M. RUST.

Marconi Wireless Telegraph Co. Ltd.,  
Great Baddow, Essex.

As Mr. Rust states, the effect of the dielectric coating is to keep the field closer to the wire and thus improve the efficiency of the launching and collecting horns. It cannot improve the transmission along the wire, for dielectric losses are added to the conductor losses, as shown in Fig. 4. We agree with the suggestion that a bare wire might be used with a tapered dielectric loading within the field of the horns; in this way a high efficiency could be obtained with relatively small horns, without any dielectric losses in the line. This assumes, of course, that the line is far enough removed from any surrounding material in which losses might be induced.

G. W. O. H.

## Amplifier with a Negative-Resistance Load

SIR,—In connection with the paper by D. M. Tombs and M. F. McKenna (*Wireless Engineer*, June 1950, p. 189), a practical application of the principle may be of interest. In *Electronics* of June 1946 I described a "Re-entrant Pentode A-F Amplifier," a resistance-coupled audio amplifier with two stages cascaded along a single electron stream. The first and second grid form a triode; the amplified voltage from the second grid is impressed upon the third grid which, together with the anode, forms another triode.

The third grid functions by distributing the space current between anode and second grid and therefore its mutual conductance with respect to the second grid is negative. A negative admittance is thus added in parallel to the load resistance of the first triode section. In normal operation, the resultant total load is negative: The voltage gain in the first triode is normally 30 although  $\mu$  is 17. These relations are described in

greater detail in the above-mentioned article, p. 124.

The arrangement was used in a hearing aid made by Zenith Radio Corporation in the United States in 1944, using the Raytheon CK511 valve which was designed especially for this circuit. To resolve any questions regarding the practicability of "larger-than- $\mu$ " arrangements, it might be noted that more than 100,000 of these instruments were successfully used in the field.

ROBERT ADLER.

Zenith Radio Corporation,  
Chicago, U.S.A.

## X-Cut Quartz Crystals

SIR,—I am disappointed that F. M. Leslie, in his paper "X-Cut Quartz Crystals" in the June *Wireless Engineer*, shows only an approximate equivalent circuit. An exact equivalent which explains the behaviour of a quartz transducer under all conditions is possible.

The conventional equivalent circuit of a quartz crystal, applicable for frequencies near to resonance, is that of Fig. 1. A. T. Starr<sup>1</sup> showed that the series LC circuit could with greater accuracy be replaced by a transmission line as in Fig. 2. This representation is valid in all cases where the acoustic loading on the active faces of the crystal is symmetrical.

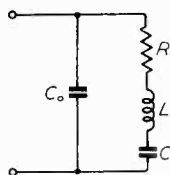


Fig. 1.

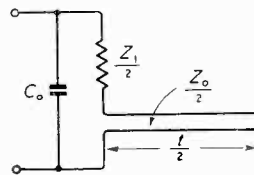


Fig. 2.

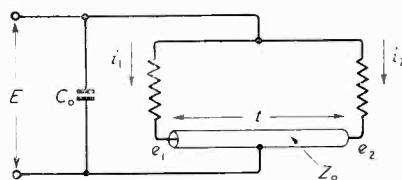


Fig. 3.

To cover the general case of unsymmetrical acoustic loading of any magnitude we have to take the circuit of Fig. 3. This consists of a transmission line of length equivalent to the crystal thickness, shown as a coaxial for clarity. The outer of the coaxial forms one of the external terminals and the two ends of the inner are taken to the other terminal via impedances  $Z_1$  and  $Z_2$ . These impedances are equivalent to the acoustic loads on the two crystal faces, respectively, and need not necessarily be resistive.

Treating the transmission line as a quadripole, the equations connecting the voltages and currents at the ends may be written:—

$$e_1 = -jZ_0 (i_1 \cot \beta t + i_2 \operatorname{cosec} \beta t) \quad \dots \quad (1)$$

$$e_2 = -jZ_0 (i_2 \cot \beta t + i_1 \operatorname{cosec} \beta t) \quad \dots \quad (2)$$

In Fig. 3 the voltage across the external terminals,

$$E = i_1 Z_1 + e_1 = i_1 (Z_1 - jZ_0 \cot \beta t) - i_2 jZ_0 \operatorname{cosec} \beta t \quad (3)$$

$$\text{also } E = i_2 Z_2 + e_2 = -i_1 jZ_0 \operatorname{cosec} \beta t + i_2 (Z_2 - jZ_0 \cot \beta t) \quad (4)$$

Solving (3) and (4) for  $i_1$  and  $i_2$  we have

$$i_1 + i_2 = E \frac{(Z_1 + jZ_0 \operatorname{cosec} \beta t - jZ_0 \cot \beta t)}{Z_0^2 \operatorname{cosec}^2 \beta t + (Z_1 - jZ_0 \cot \beta t)(Z_2 + jZ_0 \operatorname{cosec} \beta t - jZ_0 \cot \beta t)} \quad (5)$$

$$= E \frac{Z_1 + Z_2 + 2jZ_0 (\operatorname{cosec} \beta t - \cot \beta t)}{Z_1 Z_2 + Z_0^2 - jZ_0 (Z_1 + Z_2) \cot \beta t}$$

Hence the input impedance at the terminals (omitting the capacitance  $C_0$ ) is,

$$Z_{in} = \frac{Z_1 Z_2 + Z_0^2 - jZ_0 (Z_1 + Z_2) \cot \beta t}{Z_1 + Z_2 + 2jZ_0 (\operatorname{cosec} \beta t - \cot \beta t)} \quad (6)$$

$$= Z_0 \frac{Z_1 + Z_2 + j \left( Z_0 + \frac{Z_1 Z_2}{Z_0} \right) \tan \beta t}{2 Z_0 \left( \frac{\cos \beta t - 1}{\cos \beta t} \right) + j(Z_1 + Z_2) \tan \beta t}$$

If we put  $Z = z/m^2$ , this is the same as the impedance of the quartz crystal derived by F. M. Leslie<sup>2</sup>. The circuit of Fig. 3 may thus be used without any restrictions on the magnitudes of  $Z_1$  and  $Z_2$ .

It is interesting to consider how this circuit explains the behaviour of an acoustically-loaded crystal under various circumstances.

(1). If the loading is symmetrical,  $Z_1 = Z_2$ , the current and voltage distribution in the transmission line is symmetrical and it may therefore be 'folded-over' on itself producing an open-circuited line of impedance  $\frac{1}{2}Z_0$  and length  $\frac{1}{2}t$  in series with an impedance of  $\frac{1}{2}Z_1$ , which is Dr. Starr's circuit of Fig. 2.

If  $Z_1$  is resistive, at frequencies near to resonance the circuit of Fig. 1 may be used. The values which are obtained for the series LCR circuit at the fundamental resonance ( $t = \frac{1}{2}\lambda$ ) are:—

$$Q = \frac{\omega_0 L}{R} = \frac{\pi}{4} \frac{Z_0}{Z_1}; \quad C = \frac{4}{\pi^2 f_0^2 Z_0}; \quad L = \frac{Z_0}{16 f_0^2} \quad (7)$$

For example, with both faces in contact with water

$$Z_0/Z_1 = 10; \quad Q = 7.8$$

with both faces in contact with mercury

$$Z_0/Z_1 = 0.76; \quad Q = 0.6.$$

(2). If one face of the crystal could be made perfectly rigid ( $Z_2 = \infty$ ) the circuit then becomes an open-circuited line of length  $t$  in series with  $Z_1$ . The fundamental series resonance is now at  $t = \frac{1}{4}\lambda$ ; i.e., at half the normal frequency, there being an antiresonance (high impedance) at  $t = \frac{3}{4}\lambda$ .

The constants of the equivalent lumped circuit are now:—

$$Q = \frac{\pi Z_0}{4 Z_1}; \quad C = \frac{4}{\pi^2 f_0^2 Z_0}; \quad L = \frac{Z_0}{4 f_0^2} \quad (8)$$

(3). When the damping on one face is very small ( $Z_2 = 0$ ) equation (6) reduces to

$$Z_{in} = Z_0 \frac{Z_1/Z_0 + j \cot \frac{\beta t}{2} \frac{Z_1^2}{Z_0^2} \frac{\cos \beta t}{(\cos \beta t - 1)} - 2}{4 + \frac{Z_1^2}{Z_0^2} \cot^2 \frac{\beta t}{2}} \quad (9)$$

It is interesting to note the change of form of this impedance with respect to frequency when  $Z_1/Z_0$  is changed. This is shown in Fig. 4 where the reactance is plotted for various values of  $Z_1/Z_0$ . The change from a half-wave resonator when  $Z_1/Z_0$  is small to a quarter-wave resonator, when  $Z_1$  is large, can be seen.

For  $Z_1/Z_0 = 2$  it is seen that no series resonance is present at any frequency. This explains the result of an experiment where a quartz crystal was firmly cemented in a block of steel of acoustic impedance approximately twice that of quartz. Impedance measurements over a wide range of frequency did not reveal any resonance corresponding to the quartz crystal.

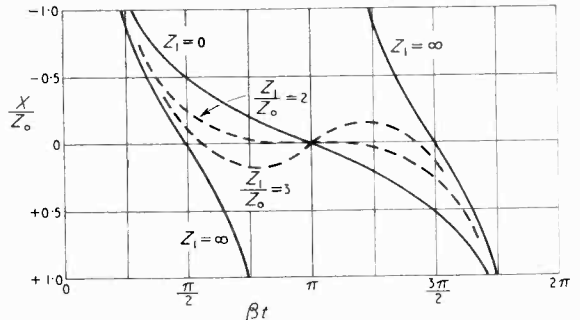


Fig. 4.

If  $Z_1$  is less than  $2Z_0$ , then at frequencies near to  $t = \frac{1}{2}\lambda$  the series circuit of Fig. 1 may be used, the constants being:—

$$Q = \frac{\pi}{4} \left( \frac{2Z_0}{Z_1} - \frac{Z_1}{2Z_0} \right); \quad C = \frac{8}{\omega_0 \pi Z_0 \left( 1 - \frac{1}{4} \frac{Z_1^2}{Z_0^2} \right)}$$

For example, with one face only in contact with water  $Q = 15$  and with one face only in contact with mercury  $Q = 0.7$ .

In conclusion, I would like to point out two errors preceding equation (4) of F. M. Leslie's article. The expressions  $-\xi'_1 S_1 = z_1$  and  $\xi'_2 S_2 = z_2$  should be  $-S_1/\xi'_1 = z_1$  and  $S_2/\xi'_2 = z_2$ .

H. GRAYSON

Standard Telecommunication Laboratories Ltd.,  
Enfield, Middx.

#### REFERENCES.

- "Electro-Acoustic Reactions," by A. T. Starr, *Wireless Engineer*, June 1940.
- "X-Cut Quartz Crystal," by F. M. Leslie, *Wireless Engineer*, June 1950.

### VELOCITY OF LIGHT

A new measurement of the velocity of light has been carried out by Dr. L. Essen at the National Physical Laboratory and it has been found that the normally accepted figure is in error by 11 miles per second. The new measurement of 186,282 miles per second confirms a previous measurement by Dr. Essen, announced in 1947, and since confirmed by other measurements in Sweden and in the U.S.A.

The determination was carried out at a radio-frequency of 10,000 Mc/s by measuring the resonant wavelength of a cavity resonator having its dimensions accurate to within one-hundred thousandth of an inch and the frequency of oscillation to 1 part in  $10^6$ . The resonator was in the form of a tube 7-in long.

### BRITISH INSTRUMENT INDUSTRIES' EXHIBITION

An exhibition of British scientific and industrial instruments is to be held in the National Hall, Olympia, from 4th to 14th July 1951. It is not confined to electrical apparatus. The organizers are F. W. Bridges & Sons Ltd., Grand Buildings, Trafalgar Square, London, W.C.2.

# NEW BOOKS

## Aerials for Centimetre Wave-lengths

By D. W. FRY and F. K. GOWARD, Pp. 172 + x. Cambridge University Press, 200 Euston Road, London, N.W.1. Price 18s.

The title of this monograph might more accurately have been "Centimetric Wave-Length Aerials for Radar." While radar applications have comprised not only the major utilization of these very high frequencies, but also the need urging the development of the appropriate technique, there is, nevertheless, an important and increasing usage in the communications field. It is true, as the authors remark in their introduction, that centimetric aerials for other applications introduce few problems not encountered in radar work, but by far the greater proportion of their book is devoted to those aerial characteristics and problems which are peculiar to radar. These include the production of specially-shaped polar diagrams, the use of long linear arrays to obtain beams narrow in one plane and wide in another, and means for scanning; i.e., cyclically varying the direction of the beam so that it sweeps continuously over a required area. Consideration of non-scanning and omni-directional aerials having little radar significance is relegated to an appendix.

The authors have assumed considerable technical knowledge on the part of their readers; in any event, few could appreciate the problems of centimetric work without graduating from lower frequencies. The quasi-optical nature of the subject is well covered, and emphasis is placed on the direct applicability of optical principles to the solution of aerial problems. Fourier analysis and other methods for the design of a radiating aperture to meet specified conditions are discussed, but the treatment is not excessively mathematical. Frequent references are given in the text where further explanation or greater detail may be desired, and a useful bibliography is included.

From an engineering standpoint, a possible criticism is that much that is important or interesting is treated rather superficially. It is less a complete exposition of the design of centimetric aerials than a record of the various types, with explanations to ensure that the objects of a design, the controlling parameters, and the manner of its achievement are appreciated.

The book is well written, with only occasional lapses into professional jargon. The explanatory diagrams are clearly drawn, and there is a notable freedom from textual and typographical errors.

C. G.

## The Theory and Design of Inductance Coils

By V. G. WELSBY, Ph.D., A.M.I.E.E. Pp. 180 with 61 diagrams and photographs. Macdonald & Co. (Publishers) Ltd., 43 Ludgate Hill, London, E.C.4. Price 18s.

This book will be welcomed by engineers in the many branches concerned with the applications of inductors, for it supplies a very definite need. The calculation and measurement of the inductance of air-cored and low-frequency iron-core coils is, of course, easy work for most designers, and Dr. Welsby has therefore devoted most of his space to the far more difficult problems of coil losses and of iron-core coils at high frequencies. In addition to collecting and adapting existing information for the benefit of the coil designer, he has contributed original work on the design of stranded wire and graphical aids. He frankly admits

that much remains to be done, and that some types of inductor (notably non-toroidal dust-core types) are not amenable to exact design, and the use of theory is mainly as a guide in interpreting and applying the results of measurements on sample coils. For this reason it must not be supposed that the design of such coils is reduced to merely evaluating formulae and reading graphs. One must have an intelligent appreciation of the assumptions and limitations involved.

After assessing the various kinds of losses in air-cored and iron-cored coils, the author applies the results in terms of  $Q$ , especially in relation to frequency. There is a chapter on harmonic distortion in iron-core coils, one on measurements (its rather sketchy nature being perhaps excusable on the ground of the abundance of existing information), and the book ends with a chapter for which the practical designer will be particularly grateful, consisting of typical examples of coil design.

The problems of eddy-current losses in conductor and core and of hysteresis losses are gone into thoroughly. Dielectric losses and low-capacitance windings receive surprisingly little attention; there is no reference at all to wave winding and similar methods. The book is sufficiently up to date to include a brief description of ferrite core materials; this will no doubt have to be expanded in later editions.

A very helpful addition would be a list of symbols, especially as one or two of them make their appearance without being introduced to the reader. A bibliography is provided, but there are very few references in the text. This is especially unfortunate in those cases where the derivation of equations is not indicated. For example, Chapter VIII is based largely on an expression introduced with the words "It can also be shown that, making certain assumptions . . .", the assumptions not being stated. There are more than a few errors, and before using equations it is advisable to check them. The definition of  $Q$ , and the symbols used to refer to it, are rather loose; and there are some discrepancies between diagrams and text.

There is no doubt, however, that this is a book that every communication engineer ought to study.

M. G. S.

## Communication Circuit Fundamentals

By CARL E. SMITH, Pp. 401 + x. McGraw-Hill Publishing Co. Ltd., Aldwych House, London, W.C.2. Price 42s. 6d.

If any type of book demands more careful writing than another, it is that which purports to teach the basis of a subject *ab initio*. As in building, sound practice requires that each brick be supported on those already laid rather than by those yet to come. Ambiguities should be strictly excluded, and statements should avoid looseness on the one hand and pedantry on the other.

The framework of the book under review is well adapted to its purpose, mainly as part of a course of home study in communication engineering. It begins with the fundamental concepts of matter and energy, and goes on to introduce electrical quantities, first in d.c. circuits. After chapters on magnetism, inductance, and capacitance, the author deals with the basic types of a.c. circuit, then network theorems, and finally the elements of valves and cathode-ray tubes. There are worked-out examples illustrating each new step, and every chapter ends with a summary of the main points and a set of exercises. About 50 pages of tables and other reference material, a full index, and answers to the exercises, complete the volume.

The actual writing, unfortunately, can on the whole only be described as slipshod. To quote some typical samples: on p.5 it is stated that "there are lines of force emanating from the proton," but there is no warning that such lines are any less real than the proton. Magnetic field intensity "is generally stated in terms of the number of lines of flux per sq cm at right angles to the magnetic field at any point . . . The ratio of flux density to field intensity is called *permeability*." "The magnetic lines of force encircling each loop of the conductor (in a coil) will move in opposite directions between each loop of the coil." "One *weber* is defined as that change in flux linkage per sec which will induce 1 volt in a single turn of conductor."

Seeing that the book is the second in a series by the same author, the first being on applied mathematics, one might expect a reasonably consistent standard of mathematics. For the most part the author avoids anything but the most elementary algebra, and often develops new ideas with the aid of numerical examples; but on p.130, the reader is switched abruptly over to differential equations as the sole means of understanding the inductive circuit; in the next chapter the analogous capacitive circuit is treated only descriptively; while farther on still four pages are devoted to dodging the calculus in showing how an elementary a.c. generator produces a sinusoidal waveform. Some equations are derived with lengthy explanation; others are stated without a hint of a proof. An example of magnetic circuit calculation, admittedly very approximate owing to the neglect of leakage flux, is worked out to five significant figures. In a diagram of a 5-range milliammeter, the line current is shown as having to pass through all the shunts in series on all ranges. The use of units is thoroughly inconsistent.

Nevertheless, some sections are very good, notably those devoted to circuit networks, in which the treatment of equivalents, circuit theorems, and reactance sketches is simple and clear. With some careful revision of the text the book would admirably fulfil its object.

M. G. S.

### Einführung in die Funktechnik

By FRIEDRICH BENZ. Pp. 736 + xx with 705 illustrations. Springer-Verlag, Vienna 1, Mölkerbastei 5. Price 78s.

This is the fourth edition of a book first published in 1937; it has been much enlarged and is a very comprehensive and up-to-date text-book of radio engineering. It is divided into five parts, of which the first, consisting of eighteen chapters, is devoted to general foundations, including a.c. principles, rectifiers, transformers, networks, Maxwell equations, modulation, piezo-electricity, dielectric and magnetic materials, etc.

The second part, consisting of seventeen chapters, is devoted to valves of all types, photo-electric cells and cathode-ray tubes. The third part, containing eleven chapters, is devoted to low-frequency amplification, electro-acoustics, microphones and loud speakers. The fourth part, containing seventeen chapters, deals very fully with receivers of all types, while the final part of thirteen chapters deals with generating and transmitting equipment, including magnetrons, klystrons and travelling wave tubes, and also aerials of various types. Every branch of the subject is dealt with both theoretically and practically with many photographs showing details of the actual apparatus.

The reader is assumed to have reached a reasonable standard of mathematical ability; already at page 11 Fourier analysis is applied to various waveforms, including the saw-tooth. The system of units employed is the rationalized system introduced by Mie, in which

the practical units, the ampere and volt, are used, but the cm is maintained as the unit of length. There is no reference to Giorgi or to the m.k.s. system. The unit of  $H$  is the ampere-turn per cm, the unit of  $B$  the weber per cm<sup>2</sup>, that of permeability the henry per cm and that of permittivity the farad per cm. There is no doubt that in many ways the cm is preferable to the metre as the unit, especially when dealing with current and flux densities. As we pointed out when discussing this system in the editorial of November 1948, since the unit of force is the joule per cm, which is 100 newtons, the unit of mass is necessarily 10 tons or 10<sup>7</sup> grams. The unit of force is also stated to be equal to 10.2 kp, i.e., 10.2 kiloponds, where a kilopond is the force equal to the weight of 1 kilogram.

We were interested to see the Edison cell referred to as the steel accumulator "because it is usually contained in a steel case," and Fig. 1 is stated to give discharge curves of lead and steel accumulators.

The book contains a great number of references which will make it valuable to a radio engineer. At the foot of nearly every page references are given to publications dealing with the subject under discussion. It is a pity that a little more care was not taken in the initials and spelling of names: J. J. Thomson becomes J. L. Thomson, J. A. Fleming becomes L. Fleming, Espley and Oatley become Esplay and Oetley and Kennelly becomes Kenelly, but these things are difficult to avoid in such a large number of references in a foreign language.

Fig. 362, which is supposed to show the nature of the electric field in the neighbourhood of a radiating aerial, is entirely wrong, and the treatment of the subject is very unsatisfactory. This may be partly due to the strange arrangement whereby reception, amplification, etc., are all dealt with before the generation and radiation of electromagnetic waves, which are reserved for the final section of the book.

Although there are over 700 pages, the author points out in the preface that, owing to the enormous development of the subject during the last ten years, it is only possible to give the more important principles of many of the newer developments, and that, in accordance with its title, the book must be regarded as an introduction. As mentioned above, however, references are always given to more detailed publications, and the book is intended to be not only a text-book for students but a reference book for the practising radio engineer. Although it contains such a large amount of material, it omits some things that a student will want to know; for example it gives formulae for the inductance of a straight piece of wire of length  $l$  and diameter  $d$ , but gives no proof of the formula or explanation of what is meant by the inductance of such a piece of wire. The same is true of the inductance of two parallel wires; the formula is given but not a word of proof or explanation, nor any reference to a book on the subject. It may be maintained, however, that the student should have obtained this information from other sources before commencing the study of radio-engineering.

The book is very well produced; paper, printing, and diagrams are all excellent.

G. W. O. H.

**Die Elektromagnetische Schirmung in der Fernmelde- und Hochfrequenztechnik.** (Electromagnetic Screening in Telecommunications and High Frequency Engineering)

By DR. HEINRICH KADEN. Pp. 274 + viii with 132 illustrations. Springer-Verlag, Mölkerbastei, 5, Wien 1, Austria.

The author is a well-known authority on this subject; he has been for many years in the laboratories of Siemens and Halske and has devoted himself specially

to the study of screening. Although he has published many papers on the subject the book contains much that has not been published. As far as possible the contents are arranged in order of difficulty.

The book is divided into two parts; the first part deals with screening against interfering fields, and the second part with screening against interfering currents in multi-core cables. An introductory section is devoted to the Maxwell equations in Cartesian, cylindrical and spherical coordinates, and at the end of the book there is an appendix with the more important properties of the cylindrical and spherical functions which enter largely into many of the screening problems. The opening section also deals with the depth of penetration and equivalent thickness of the conducting layer due to skin effect. The first chapter deals with closed screens with homogeneous walls, first with the disturbing magnetic field outside the screen and then with it inside the screen, with single screens and with screens of several layers of different metals. The second chapter deals with screens that have breaks in the metallic continuity in various directions, but no openings; screens with definite openings and gaps are dealt with in the third and fourth chapters. The fifth chapter deals with the electric and magnetic screening effect of grids and networks. The second section of the book is devoted to screening against cross-talk due to currents in neighbouring cores in telephone cables of various constructions.

The treatment throughout is very thorough and necessarily of a mathematical character as many of the problems involve Bessel and Hankel functions. The bibliography contains 49 references to papers on the subject.

Fig. 19 is somewhat puzzling until one realises that it is upside down. The word 'kreis' under Fig. 68 should be 'kreis'; there have been several accidents with the type on the same page, and on p. 269 there is a reference to a paper on the 'industance and retisance' of coils. These are minor details, however, and the book is undoubtedly a valuable addition to the literature on this subject.

G. W. O. H.

#### Graphical Symbols for Telecommunication—Component References.

Supplement No. 1 (1950) to British Standard 530: 1948. Pp. 12. British Standards Institution, 24/28 Victoria St., London, S.W.1. Price 2s.

Previous editions of B.S.530 have not contained any directions for identifying components in a diagram. In the 1948 edition it was stated that the matter was being discussed among interested parties. Difficulties were due to the different methods adopted by telephone engineers on the one hand and radio engineers on the other, but the increasing intermingling of telephone and radio circuits made it necessary to come to some agreement. The result is a compromise, reducing to a minimum the changes to be made in each system.

Components are divided into two classes:—  
(a) Switches, relays and similar devices, and (b) All other components.

All components are designated by one or more letters; several similar components are distinguished in class (a) by the addition of A, B, C etc. and in class (b) by the addition of 1, 2, 3, etc. Thus, three switches would be SWA, SWB, and SWC, whereas three transformers would be TR1, TR2, and TR3. If the switch SWB has several contact units they will be SWB1, SWB2, etc., whereas in class (b) if the transformer TR2 has several terminals, they will be TR2a, TR2b, etc. It seems a pity that a common system could not be adopted for both classes.

The supplement contains tables giving the designations of the various components, and the class, to which they belong. Some are mandatory, some optional, and permissible exceptions are explained.

G. W. O. H.

#### Glossary of Terms used in Radar.

Supplement No. 4 (1950) to British Standard 204: 1943. Pp. 12. British Standards Institution, 24/28 Victoria St., London, S.W.1. Price 2s.

The 1943 'Glossary of terms used in telecommunication' is naturally incomplete in those fields in which there has been great development in recent years. A number of supplements are being issued dealing with the terms used in these fields. In this supplement the first section deals with nine terms that are not peculiar to radar, and the second section with forty-nine terms that apply only to radar. In some cases a number (in one case five) of deprecated alternative terms are given. To anyone not well acquainted with the subject, some of the terms, such as snow, grass, jitter and clutter will seem strange, but it is important that those who are engaged in radar operation training and research should know the exact meaning of the various terms and also which to employ when there are several alternatives.

G. W. O. H.

#### Radio Servicing

By ABRAHAM MARCUS. Pp. 775 + xxi. George Allen & Unwin Ltd., 40, Museum St., London, W.C.1. Price 35s.

This book covers elementary theory as well as servicing. It is of American origin and so the apparatus taken as examples and, in particular, the test equipment described, are all of American type.

#### Radio Laboratory Handbook

By M. G. SCROGGIE, B.Sc., M.I.E.E., 5th Edition. Pp. 430 with 215 illustrations. Hiffe & Sons Ltd., Dorset House, Stamford St., London, S.E.1. Price 15s.

#### Theory and Application of High Frequency Phenomena

Edited by Y. ASAMI. Pp. 68. Research Institute of Applied Electricity, Hokkaido University, Sapporo, Japan.

#### Electronic Engineering Master Index, 1949

Pp. 296 + xvi. Electronic Research Publishing Co. Inc., 480, Canal St., New York 13, U.S.A. Price \$17.50.

#### Air Compressors

By P. C. BEVIS. Pp. 192 + vii with 87 illustrations. Sir Isaac Pitman & Sons Ltd., Kingsway, London, W.C.2. Price 20s.

#### The Patents Act 1949

Pp. 327. Sweet & Maxwell Ltd., 2 and 3, Chancery Lane, London, W.C.2. Price 37s. 6d.

### ELECTRICAL TECHNICIANS

The Institution of Electrical Engineers has published a report on "The Education and Training of Electrical Technicians," which is obtainable from the Institution, Savoy Place, London, W.C.2. Price 1/-. The report is that of a committee appointed by the Council of the British Electrical & Allied Manufacturers' Association, The Radio Industry Council, and the Council of the I.E.E.